Executive summary

This project is carried out in the framework of a contract between the "Water and Environment Centre" (University of Sana'a, Yemen) and the International Institute of Aerospace Survey and Earth Sciences (ITC-Enschede, The Netherlands), as part of the Sana'a University Support Project funded by The Netherlands Government. This study is partly financed by the WB, Rural Development, Water and Environment, Middle East and North Africa Region.
The study took place from early March 2000 to middle of March 2001. Field data were collected during the period March 2000 to March 2001.

The main results of the remote sensing (Landsat TM) study are:

The acreage of qat, grapes, mixed cereals & other and fruit trees during summer in the year 2000, when ground-truth data sets were available, for the entire Sana'a basin is shown in the table below. For the sake of comparison, the estimated irrigated acreage, as derived by remote sensing, for the years 1985,1989, 1994, 1995 and 1998 are included in the report.

Crop	Acreage (ha)
Qat	10300
Grapes	9130
Mixed cereals & other	3530
Fruit trees	420
Total	23380

A 1: 100,000 scale map with the crop types is included.

The development of irrigated areas since 1985 is shown in the table below. A map showing the distribution of the irrigated areas is included.

Date	Irrigated acreage (ha)		
09-03-1985	9000	-	11000
12-05-1985	11000	-	13000
06-10-1989	13000	-	16000
12-10-1994	21000	-	25500
16-01-1995	15000	-	19000
24-05-1995	24000	-	29500
01-06-1998	24500	-	30000
26-03-2000	16500	-	20000
13-05-2000	21000	-	25500
12-10-2000	25000	-	30500

Actual evapotranspiration of the irrigated crops was calculated by using surface energy balance equations at three dates in the year 2000.

It was found that the actual evapotranspiration rates of irrigated areas vary widely. If the important areas for qat and grape cultivation are considered, e.g. Wadi As Sirr and Wadi Dhar, ETa values are generally in the

range of a few to 5.5 mm per day. By summing up the total ETa rates of cropped areas (mostly irrigated), in combination with long-term average crop reference transpiration, the *maximum* amount of water used by irrigated crops works out to be between 60.6 and 75.1 million m3 for the year 2000. Using an irrigation efficiency of around 40%, this means a yearly total of between 150 and 190 million m^3 water is used for irrigation.

The report contains statistics on crop types, irrigated acreages and evapotranspiration by crops per sub-catchment.

Study of lineaments on satellite images suggest that no important quantities of groundwater leave Sana'a Basin along the western, southern and eastern boundaries. It is likely that groundwater escapes along the northern boundary, but this requires confirmation by head data and other hydro geologic studies. Evidences on the images so far, suggest limited losses.

A map with lineaments and terrain units linked to relative recharge is included.

Along the western margin a small rift-like structure is found, which influences the sub- regional and local hydro geology. A fairly even distribution of the larger lineaments (fractures) was found. Preferred directions occur only in limited zones. Therefore, constant values for the secondary permeability can be adopted in regional groundwater modeling.

CONTENTS

Tables

Figures

1. Introduction.

1.1 Project background.

This project concerns the use of satellite data in the framework of a water management study of the Sana'a basin.
A main data need pertained to the use of groundwater by irrigated crops and its trend over the years and to work out strategies for saving irrigation water use, against the background of the mining of groundwater which is currently taking place in the Sana'a Basin.

The water use for irrigation is an important component of the water balance. Hitherto only estimates based on field reconnaissance surveys were available, whereby total acreage was estimated as well as the water use for various crops. By using satellite data, improved data can be obtained.

During the project preparation phase, the following objectives are identified:
- Irrigated areas by crops determined by RS,
- Actual crop water use determined by RS,
- Seasonal and yearly changes of the areas irrigated,
- Hydrogeologic interpretation of the images, emphasizing recharge conditions

The time period for the execution of the study was set between February 2000 and January 2001.

1.2 Relevance of the study and adjustments to local conditions

The methods for mapping the acreage and classifying the types of crops using multi spectral satellite data has been well established since the late 1970's. However, in the Sana'a basin usually the irrigated and cropped fields are very small, often much smaller than the spatial resolution of the Landsat TM 5 and 7 multi spectral sensors (28 x 28 m). This results in many "mixed pixels", composed partly of irrigated crops and partly of bare soil. A special procedure, as described in later sections was developed to minimize the effects of the mixed pixels.
This procedure included the use of NDVI transforms (see also Paragraph 2.2.1), that were also used for the determination of the irrigated acreages during the season and for different years.

A more recently developed method allows the calculation of the actual evapotranspiration using surface energy balance equations. For each pixel, the daily actual evapotranspiration (Eta) can be calculated in mm/d., yielding spatial overviews during satellite overpasses during the cropping season. The method requires the measurement of the incoming radiation and for that purpose a pyranometer attached to a data logger was installed. Therefore, an accurate calculation of Eta was only possible for the year 2000, although estimates were made for the historical period 1985 -2000.
Theoretically the actual evapotranspiration at least equals the amount of groundwater pumped. A conveyance loss and return flow (i.e., passage of water below the root zone) has to be added to obtain the groundwater draft. Generally, an irrigation efficiency of 40%, personal communication Bob Angier, World Bank, is applicable in these type of areas. Using these rates, the amount of 60 to 75 million cubic meters transpired by the crops converts to a yearly amount of between 150 and 190 million m^3 water pumped. However, many pixels have low ETa rates, which could be due to rainfed or low irrigation application in part of the basin (Southern parts), which is only valid for spring. Most is irrigated, thus effects on water use statistics are very marginally.

The results of a study of this nature can therefore be considered as an improvement of the knowledge of the water use by irrigation and the spatial pattern in the Sana'a basin.
Any plan for water management needs this information concerning a prime factor of the water balance, as well as the information of where, what crops are grown.

Also it is possible to obtain crop water use factors (F A O's kc factors) from the ETa derived by satellite data for the various crops and study the spatial variation (Mekonnen and Bastiaanssen, 2000). In case of working out of Kc factors in more detail is desired by using satellite data by a separate study, more detailed field measurements within irrigated fields are required during overpasses.

Although the estimation of Kc factors formed no part of the TOR of this study, they have been considered for the sake of validation by comparison.

Furthermore, the data on water use by irrigation is of prime importance for updating groundwater models.

The images have also been used to study the lineaments in relation to the hydrogeology of the basin, and to assess the relative recharge. Possible outflow of groundwater from the basin was of special interest. The map showing relative recharge and lineaments is also digitally available and is metrically fully compatible with the existing topographic maps.

Finally a map on I: 100,000 scale of the entire basin is produced, showing the irrigated crops with a satellite image as background. This map is also available digitally and is geometrically corrected. It can therefore be used as a base map for further studies by plotting other data, such as wells. The recent expansion of Sana'a City can be observed on the map.
The hydrologic database of NWRA can therefore be merged with the map, for further hydrological studies.

All data are available in digital form for further GIS work at WEC/NWRA, Sana'a, Yemen. The outline of the Sana'a basin is shown in Figure 1.

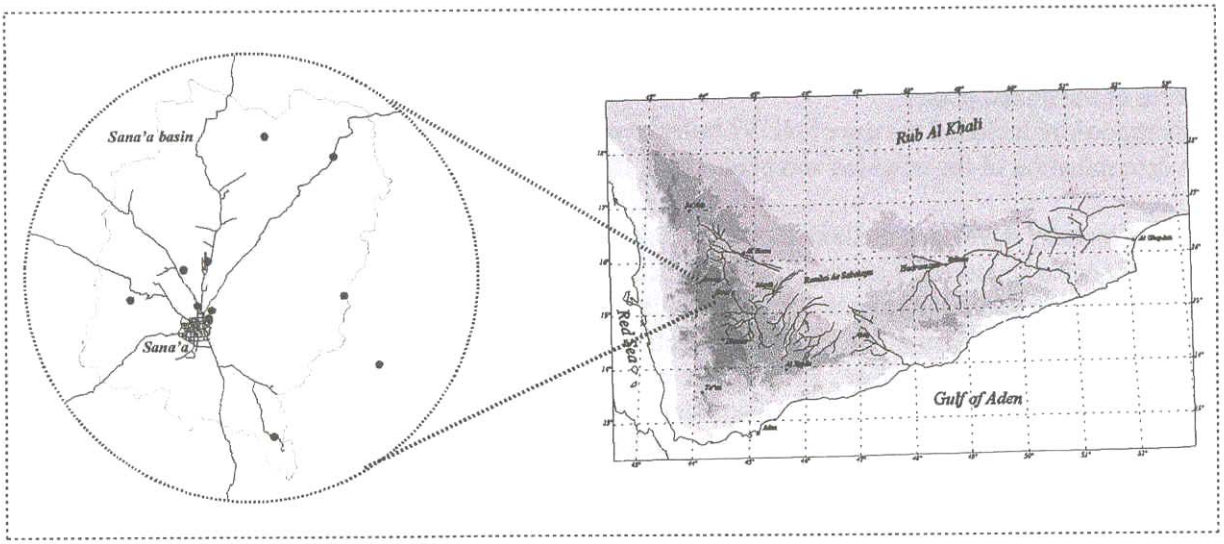

Figure 1. Project location.

PART I. CROPPING PATTERN, IRRIGATED AREAS AND ACTUAL EV APOTRANSPIRA TION BY REMOTE SENSING METHODS

2. Methods.

2.1 Crop identification.

2.1.1 Classification method.

The classification and mapping of crop types by multi-spectral satellite data is common practice since the 1970's when the first Landsat data became available (1972).
The method consists of obtaining sample sets, based on "ground-thruth", i.e., selection of pixels (picture elements) for which the crop type or surface cover is known. Statistical or other classifiers are then used to transform the entire image into a crop type of cover map. Accuracy assessment is a standard practice. Obviously, the best results are obtained when the images correspond to the time when the sample sets are obtained in the field (July 2000 in this case).

The images are geometrically rectified so that they match fully topographic maps and that GPS readings in the field can be plotted accurately. Topographic elements such as roads, etc. have been added to the images to ensure readability and location.

Various multi spectral classification methods can be used and have been tried out for selection of the one, which gave the most accurate result. Here, this is the maximum likelihood classifier.
Based on field sample sets, statistical distributions of spectral data for each cover class are calculated. After that all the pixels in the image are compared with the distributions, and a decision is made as to whether they are likely to belong to one of the classes or not. This decision makes use of a threshold value, which has to be set. Narrow values results in many unclassified pixels (a likelihood criterion is more strictly applied). A broad threshold leads to more mis- classified pixels and consequently to less accurate statistics concerning the cover classes.

As mentioned earlier the small sized irrigated parcels cause the "mixed pixel" problem. Therefore much attention was devoted to the selection of the field sample sets and a procedure was developed to calibrate the threshold values of the maximum likelihood classifier against the total irrigated area, as determined by using NDVI transforms. No straightforward classification of irrigated areas utilizing the latter images can be done under such conditions of very small fields, again because of the "mixed pixel" problem. The way this was done is discussed further on in this report. The crop classification was done by matching the threshold value in such away that the total irrigated area by multi spectral classification agrees with the total irrigated determined by the ND VI method.
A crucial element of the success of the multi spectral classification is that the crop cover classes (e.g., qat, grapes, etc.) correspond to distinct spectral classes. In case of spectral overlap of two or more cover classes, the accuracy of classification is reduced, depending on the degree of overlap (or spectral similarity).
In case of strong overlap, cover classes have to be merged.

In this study fortunately the main water consuming crops, namely qat and grapes can be spectrally differentiated and both of them can be separated from the other classes, which pertain to minor crops, such as cereals, vegetables and orchards. Because of overlap the minor cover classes cannot be classified as accurately as the major classes, and there is much to say for combining them.

The feature space of Figure 2 illustrates the separation and overlap of the clusters. The diagram shows only two spectral bands, for the classification procedure six spectral bands are used, although some of them are correlated to each other (Figure 2.b.). Bands 3 and 4 of Landsat-TM are designed for determination of vegetation characteristics. For the crop classification the 6 TM bands were used in a multi-dimensional classification, for each dilate. Also, the combination of bands 3 and 4 merged for different dates have been used, as will be discussed later .

The accuracy assessment of the classification is done by comparing the classified results with an independent data set collected in the field for comparison purposes (not the set used for the classification!) Usually a contingency table is employed for the accuracy assessment, which is provided in Paragraph 3.2.2.

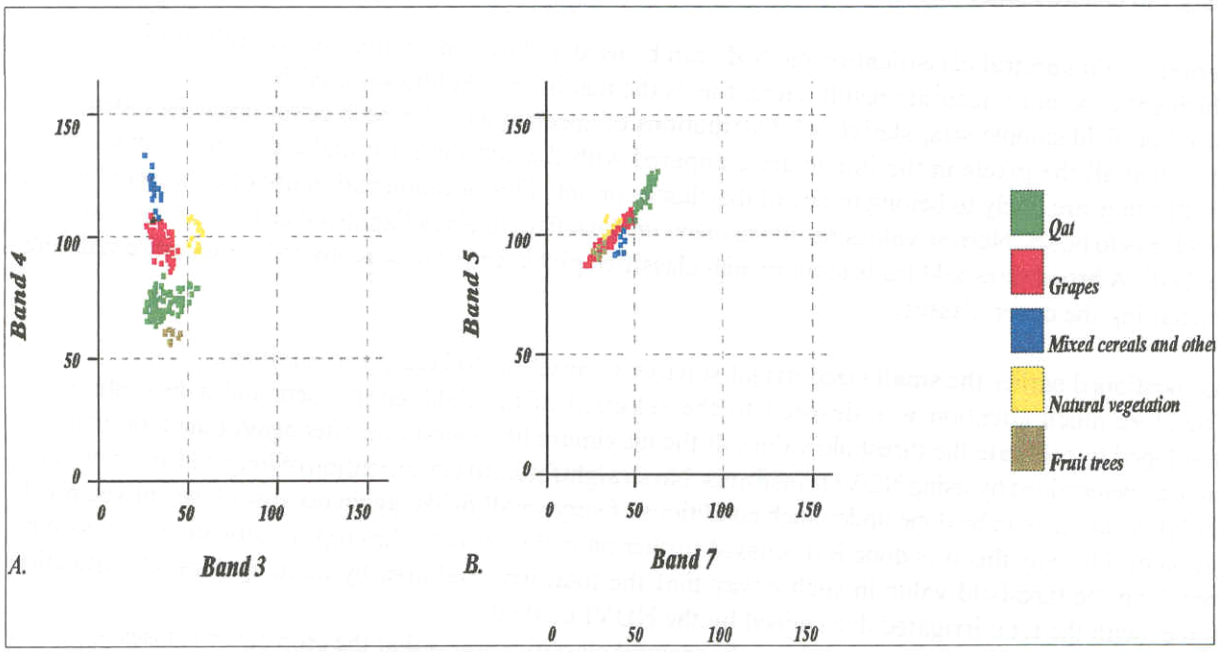

Figure 2. Feature spaces ofLandsat-1M bands 3 and 4 (A) and bands 5 and 7 (B), showing the spectral responses of the different ground cover classes.

All results are presented in Chapter 3.

Remarks about classification:
In the Sana'a basin generally qat and grapes are grown in relatively large-size fields. Other crops (potato, tomato, alfalfa, sorghum. etc.) occupy often smaller parcels and can be adjacent to either bare soil or qat or grapes. Thus. the mixed pixel problem affects mainly the crops on the smaller parcels.

Variable cropping cycles and growth stages complicate the use of spectral data sets taken at times different from the satellite overpass. For example. grapes. and as it seems also qat to a minor extent. are kept in a semi-dormant stage until they are considered to be productive after which they are heavily irrigated and ready to produce in a few weeks time. Cereals and vegetables start to grow early in the season and occur in different growth stages in different plots.
Therefore, the spectral properties of the sample sets vary with time.
Despite such complications, qat and grapes can be differentiated from other crops.

In order to improve the accuracy of the crop type classification, the sample training set was augmented by samples of about an extra 150 locations, after the first results were presented. The adjusted figures are mentioned in this report.

This problem is solved by using a multi-temporal classification image data set. For example qat will give similar, relatively high, ND VI responses over the entire year, whereas grapes basically yield high responses from say May till September, October.
Cereals and vegetables plots show another characteristic response over time, depending on crop-type and cropping cycle. Therefore the mixed cereals and vegetable les are clustered into different sub-classes, without necessarily knowing the actual crop type, in order to be able to separate them spectrally from the major classes. After running the classification procedure they are grouped into 1 class again, "Mixed cereals and other".

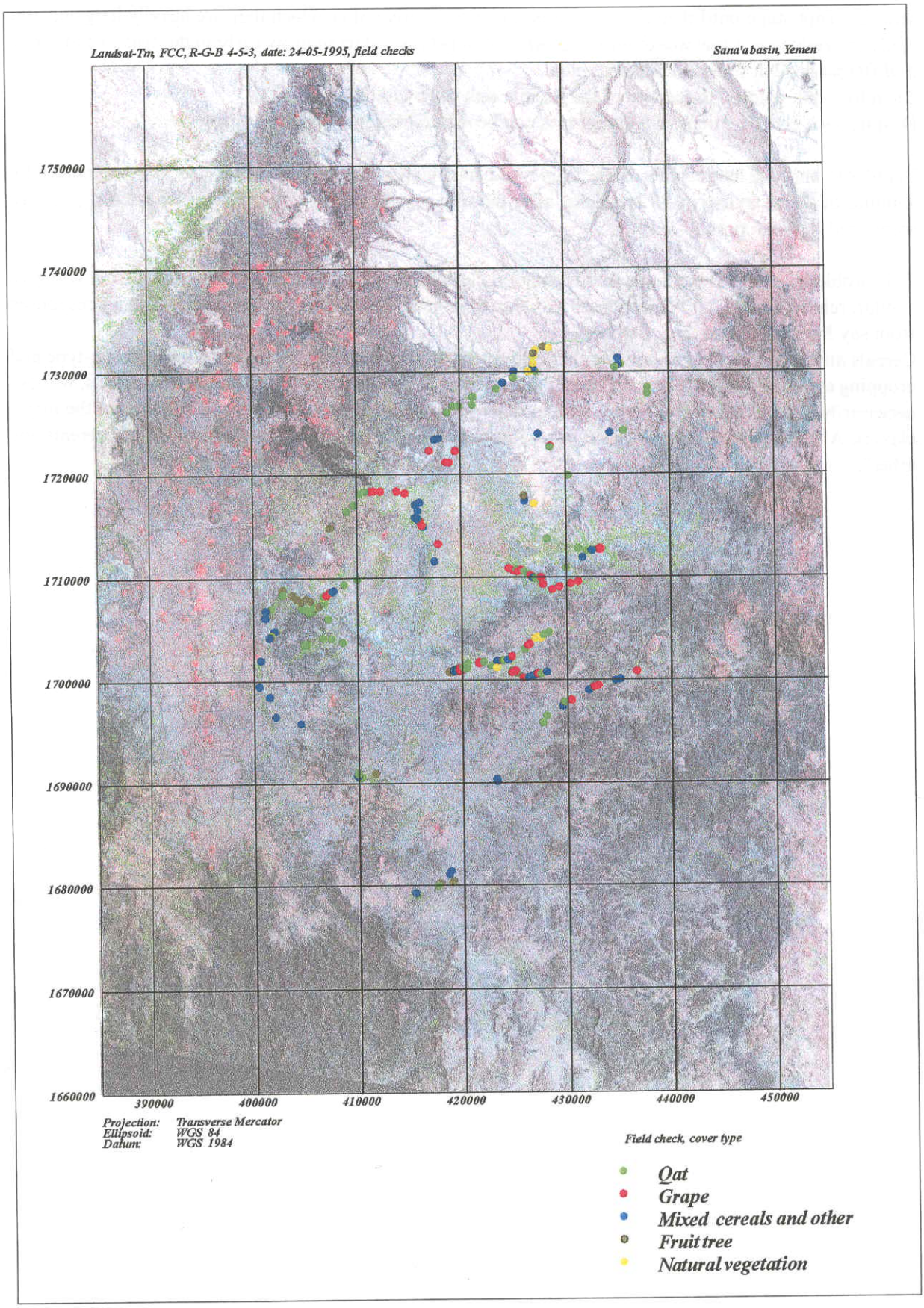

Figure 3. Location of the field traverses.

2.1.2 Field data set.

The following classes have been sampled in the field (x-y coordinates, type and period of collection are shown in the Appendix): qat, grapes, cereals and vegetables ("creals and other"), horticulture (fruit trees") and natural vegetation. In total 265 sites were visited in the field for inclusion in training sets for the multi-spectral classification.

2.1.3 Images used

The availability of cloud free images for the year 2000 covering the cropping cycle, was limited to three only.
Since a proper crop classification requires a field data set, only the three available images of the year 2000 have been used, of the following dates: 26-03-2000, 13-05-2000 and 12-10-2000.

For the historical data in the period 1985-1999, no sample sets are available. However, for the grapes and qat class, field enquiries learned that the lifetime is long (20 years and more). Hence, the sample set of the year 2000 can be applied with reasonable accuracy, for these classes. However, no accuracy assessment is possible.

The historical data made use of the Landsat TM 5 satellite of the following dates:

- 09-03-1985
- 12-05-1985
- 06-10-1989
- 12-10-1994
- 16-01-1995
- 24-05-1995
- 01-06-1998

Some additional images might be acquired, but were not purchased here. First of all, most of the (limited) images available pertained to certain periods in the year only, therefore they were considered not to give reasonable additional information concerning seasonal variation. Secondly, and not less important, there were the financial constraints.

2.2 Irrigated areas.

Determination of irrigated areas is much more simple than crop type identification, because there is much spectral contrast between lush green crops and their drier surroundings. However, rainfed crops in good condition, after rainfall prior to the satellite overpass in spring can be classified as irrigated areas. For example the satellite overpass recorded the initial growth stage on irrigated lands, but it could also be the presence of green rainfed crops or even presence of a tree canopy in a pixel, which is otherwise bare.

Attention to this aspect however is given, confusion will be only in late spring. However, interviewing local farmers during the fieldwork, learned that such is no common practice for qat and grapes. Cereals and vegetables, however, at times make use of precipitation. This is basically found in parts of the southern region of the basin (southern part of Wadi Harad al Ghayl Zahr, Wadi Ghaber al I'shash, Wadi Hizyaz Ghayman and Wadi Shahik al ajbar Sha'b).

2.2.1 NDVI transform

The NDVI transform provides a suitable image for the determination of the irrigated areas. This transform makes use of the large difference in reflectivity between the near infrared band (NIR) and the red band (RED) of green crops, whereas the difference in reflectivity of non vegetated areas is small-

$$NDVI = (NIR - RED) / (NIR + RED)$$

Radiometric sensor corrections were made because of a change of the sensors of LANDSAT 5, prior to the year 2000 and LANDSA T 7 for year 2000. A simple atmospheric correction was applied by shifting the histograms of the NIR and RED bands to their origins.

2.2.2 Classification of irrigated surface by weighted pixel method

Census data based on field surveys or cadastral data classifies the land use or irrigated field by the parcel or ownership boundaries. Therefore, all non-cropped or irrigated parts within the parcel or ownership, such as paths, yards, bare areas, etc., is classified as "crop" or "irrigated".
The satellite sensors record the actual spectral response of the crops, measured vertically above the terrain. Therefore, if within a parcel, classified in a field census as "irrigated or "grapes", only, say, 60% consists actually of green irrigated crops, then the NDVI response will be less as the response of a field where 90 % is covered by green crops.

Hence, when viewing the statistics, presented in chapter II, it should be remembered that census data will be always higher than data derived by satellite.

However, for the parcels which are occupied by fairly dense crop (say, >80% coverage) in this study the , satellite data will match a field census in the classical manner. This was achieved by using the "upper threshold", see below.
For the fields with lower green leaf coverage, the statistics based on satellite data will be much less than those of a field census.
This effect is evident when the satellite based statistics of early cropping period are compared those later in the season, when the crops are full-grown and have maximum leave development.

There are also pixels with a green leave cover, of which a variable portion consist of more than one irrigated crop. However, the NDVI response will vary linearly with the proportion green crop (i.e., irrigated) and use is made of this property for calculating the total irrigated area in m2. This mixing problem only affects the crop type statistics.

Below a certain NDVI value no green crops are found. This value -the *lower threshold*- is determined by checking the NDVI values for many pixels, known to have no green crop at the time of overpass (rock outcrops, etc.).
An *upper threshold* needs also to be defined, i.e. pixels with NDVI values exceeding a certain value is considered as fully irrigated. This is so because any field fully planted and irrigated may not cover the ground fully, when observed vertically looking down. The NDVI value is sensitive to a leaf area index (LAI) of about 3, after that NDVI values saturate. Only tall qat bushes with dense foliage and planting density will have LAI>3. The upper threshold describes therefore any pixel which is fully planted with green crops, but variations in LA! are not considered.
Between the lower and upper threshold a linear function is applied. Hence, proportions of green crop in each pixel is calculated and the result is summed up. To this, the surface area occupied by pixels fully planted with green crops, is added to yield the total irrigated area.
Figure 4 shows a small part of the NDVI image. The dark pixels have no green crops, the white pixels are fully covered. By inspecting the pixel NDVI values (clicking the cursor on the screen) of the white pixels, quite some variation of NDVI values is found, for reasons explained above.
The pixels with medium grey tones have a partial cover, as can also be deducted from the proximity relationships and by inspecting aerial photographs.
For each image, the upper and lower thresholds were determined. These thresholds, when checked in various parts of the Sana'a basin, turn out to be constant for a given image date. Therefore, for each date the total irrigated area can be calculated quite accurately.

2.2.3 Images used.

The trend in irrigation development was determined by performing the above procedure to each of the historical satellite images (see Chapter 3 for results).
The images used have been listed in section 2.1.3

2.3 Actual evapotranspiration.

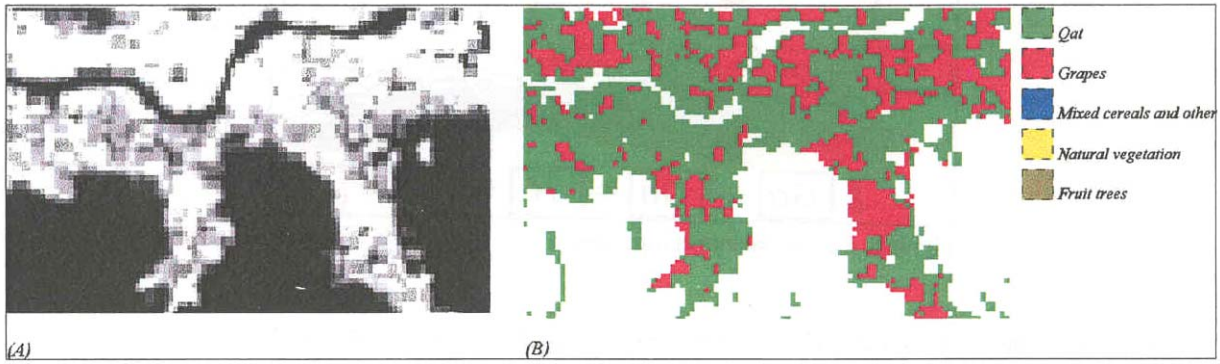

Figure 4. Examples of the determination of the irrigated areas. (A) Part of the NDVI image, (B) Same part but then showing the result from the crop classification.

A new development is the use of satellite data to calculate the actual evapotranspiration (ETa) flux from the earth surface, for each picture element (pixel). The method is quite complex because all the components of the energy balance have to be assessed. In fact, the evaporation flux is calculated by determining the other terms of the energy balance.
Developments over the last decade make it now possible to apply the method in practice on the condition that radiation data is available for atmospheric and radiometric corrections. Furthermore, air temperature data must be available.

The method used is termed "Surface Energy Balance Algorithms for Land, SEBAL "(Bastiaanssen 1995, 1998a,b).
The breakthrough is that actual evaporation can be calculated over large areas, with high spatial detail

(each and every field). Many projects all over the world now make use of the method, not only for improving water balances and irrigation management, also for crop yield predictions. In the study of the Sana'a Basin, the data will give direct information on the amount of water used by the irrigated crops. However, this is NOT the amount of water pumped! Still corrections for the irrigation efficiency (conveyance losses) need to be made, see also Paragraph 2.4.

2.3.1 Theory.

Using RS techniques for actual evapotranspiration, Ea, determination comes down to solving the Energy Balance at the Earth's surface (EBE). The EBE is the physical expression of the balances of incoming and outgoing fluxes in the boundary layer of the atmosphere.
The net radiation is the resulting difference of the incoming solar, shortwave, radiation and atmospheric, longwave, radiation and outgoing reflected, shortwave, and thermal radiation. The physical treatment of this energy requires the subdivision of net radiation shortwave and longwave incoming and outgoing radiation, Figure 5.

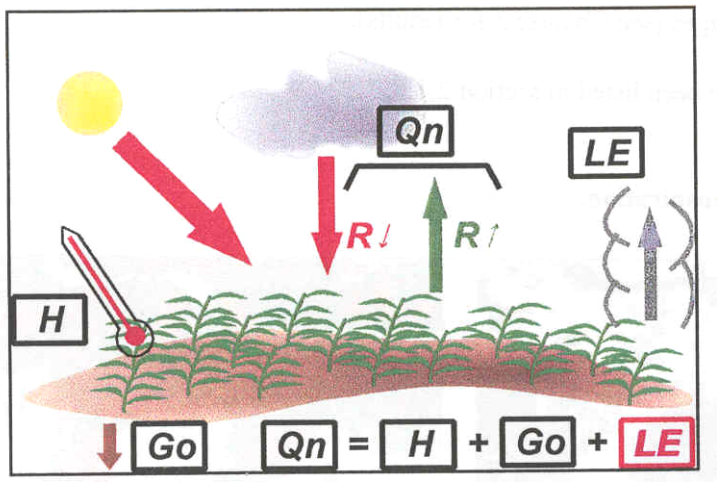

Figure 5. Energy balance components.

The resulting balance is the net radiation; the energy available for the processes to:

evaporate water (LE),
heat up the surface (H), or
to transfer energy to the soil (G).

The partitioning of the energy is ruled by the availability of water for evaporation.
Two types of energy sources are available to the system. The sun emits mainly in the shortwave range, and the atmosphere emits mainly in the thermal range of the electromagnetic spectrum.
Solar radiation reaching the ground shows wavelength ranges from 0.3 till3 µm, which is called shortwave radiation. Atmospheric components like ozone, water vapor and other gasses absorb radiation (or, energy). The different satellite channels are affected by the absorption for which the measurements have to be corrected.
Thermal radiation is produced by heated up terrestrial objects like the atmosphere and the earth's surface, where the amount of emitted radiation depends mainly on the body temperature of the object.

The net radiation simply is a summation of the incoming and outgoing shortwave and long wave radiation at the earth's surface.
Usually the net shortwave (incoming minus outgoing) radiation is determined by using the so-called albedo, or reflection coefficient. It is generally measured from the combination of the visible bands of the satellite after atmospheric correction. It can also be estimated from a reclassification of existing thematic maps, using known reflection coefficients.

The global radiation, QN' is the incoming shortwave radiation. Basically it depends on the atmospheric optical properties and the relational geometry between the sun and the earth. Usually it can be measured by one ground station pyranometer, because of its low spatial variability .
As stated before, the long wave radiation mainly depends on the body temperature of the emitting object. In the incoming case this is the temperature of the atmosphere, the air temperature, and in the outgoing case this is the earth's surface temperature, To. This surface temperature is provided by the satellite after an atmospheric correction is applied to the thermal channel. Furthermore, the amount of long wave, or thermal, radiation depends on the so-called Stefan-Boltzmann constant, a, and on the emissivity, £, which stands for the emitting ability of an object.

Since polar orbiting satellites basically provide information at one specific moment, the surface fluxes obtained from remote sensing are characterized by an instantaneous time-scale. The daily surface flux density have to be obtained by a time integration of the instantaneous surface flux densities. However, since $\lambda E/Q_N$ cannot be assumed constant throughout the day, the daily AE cannot be reliably estimated from one single AE value.

The energy partition between Hand AE is hydrological controlled and the available soil moisture changes slowly. It is therefore that so-called moisture indicators are used for revealing the energy partitioning for longer time spans. One of these moisture indicators, the evaporative fraction (A), is defined as:

$$\Lambda = \frac{\lambda E}{\lambda E + H} \qquad (1)$$

Shuttleworth, e.a.., 1989, published the first indications that A is a fairly constant indicator of energy partitioning during day light hours. Due to A(t) skewness at sunrise and sunset, a systematic difference can be found between Λ_{day} and Λ_{Right}; Λ is therefore quasi-constant during daytime only. However , Shuttleworth, e.a., .1989, compared midday Λ-values to all day Λ-averages. Because the largest contribution to λE_{24} is delivered during midday hours when Λ is constant at large radiation flux densities, the only difference was .1.5%.
The temporal stability of Λ in heterogeneous terrain and at large scale was demonstrated to be by far superior to other moisture indicators in HAPEX-EFEDA by Bastiaanssen, e.a., .1995, reason for which it is also implemented in the SEBAL algorithm, which is the algorithm used in this study.

The physically based algorithm combines ground-based and Remote Sensing information (Bastiaanssen, 1995). However, the algorithm, which uses some semi-empirical relationships, is used in such away that intensive ground measurements are avoided. For a detailed description of the algorithms used, one is referred to Bastiaanssen, 1995 and Bastiaanssen, e.a., 1998a,b.
However, the necessary ground measurements comprise, among others, the recording of incoming radiation, air temperatures (used to obtain incoming longwave radiation) and clear-sky transmissions, are obtained from pyranometer data.

2.3.2 Practical implementation

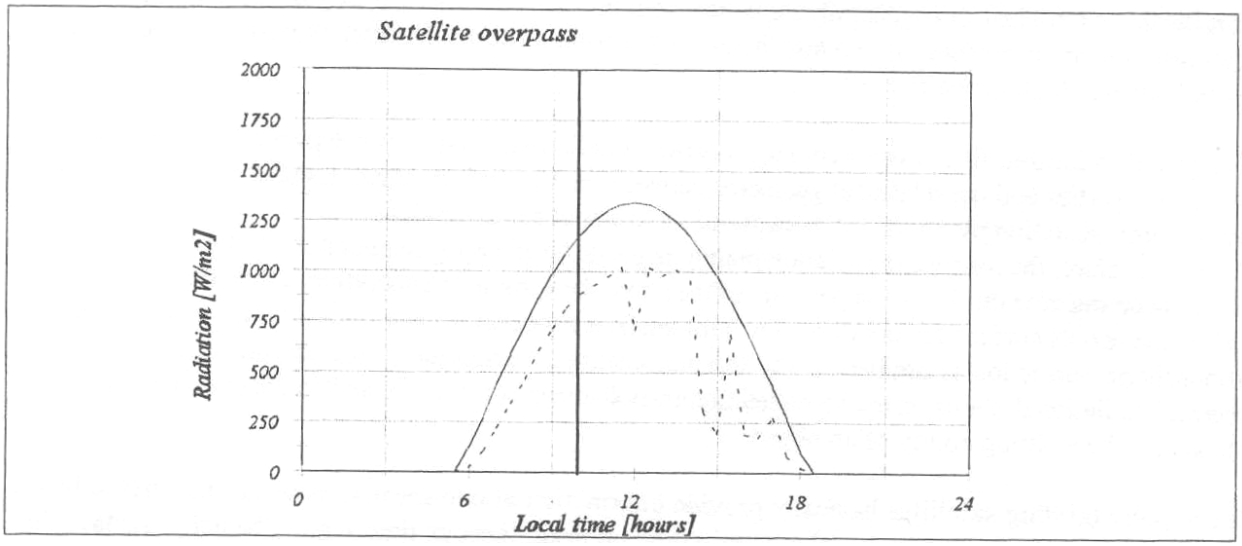

Figure 6. Example of atmospheric transmittance calculation for the shortwave radiation, for the WEC site as measured on 13 of May 2000 by a Pyranometer. Data is stored every half an hour.

Continuous recording of shortwave radiation data is done by a pyranometer installed at the WEC in February 2000, necessary for atmospheric correction. However, some additional measurements have been carried out during the fieldwork campaign on some characteristic sites in Wadi As Sirr. This site was selected because amongst other crops, typical, homogeneous ground cover of grapes and qat are present. These necessary ground-truth measurements on surface temperature have been carried out during Landsat satellite overpasses. Unfortunately, only a few images of Sana'a Basin were recorded during the overpasses.

2.3.2.1 Shortwave radiation.

To facilitate atmospheric correction for the shortwave satellite imagery continuous measurement of incoming shortwave radiation was performed at the WEC site. Figure 6 shows an examp1e of the incoming radiation during a day. The sudden drops are due to cloud overpasses.

Since the atmospheric correction scheme applied here for the shortwave radiation mainly depends on the incoming shortwave, or solar radiation, received at the earth's surface, a one-point measurement suffices. This holds true because the incoming so1ar radiation is only governed by large-scale atmospheric or earth-sun geometric relations.
The atmospheric correction, or atmospheric transmittance is then obtained by dividing the value for the measured incoming shortwave radiation (irregular curve) at the moment of satellite overpass by the incoming radiance at the top of the atmosphere (the smooth curve). In this case the atmospheric transmittance equals 0.75 on that day. From the irregular pattern it is clear that clouds are starting to develop around noon.

2.3.2.2 Thermal infrared (Iongwave) radiation.

A hand held thermal infrared radiometer was used to measure the surface temperature to facilitate atmospheric calibration of the thermal images. An example of the results of the measurements at the site is shown in Figure 7.

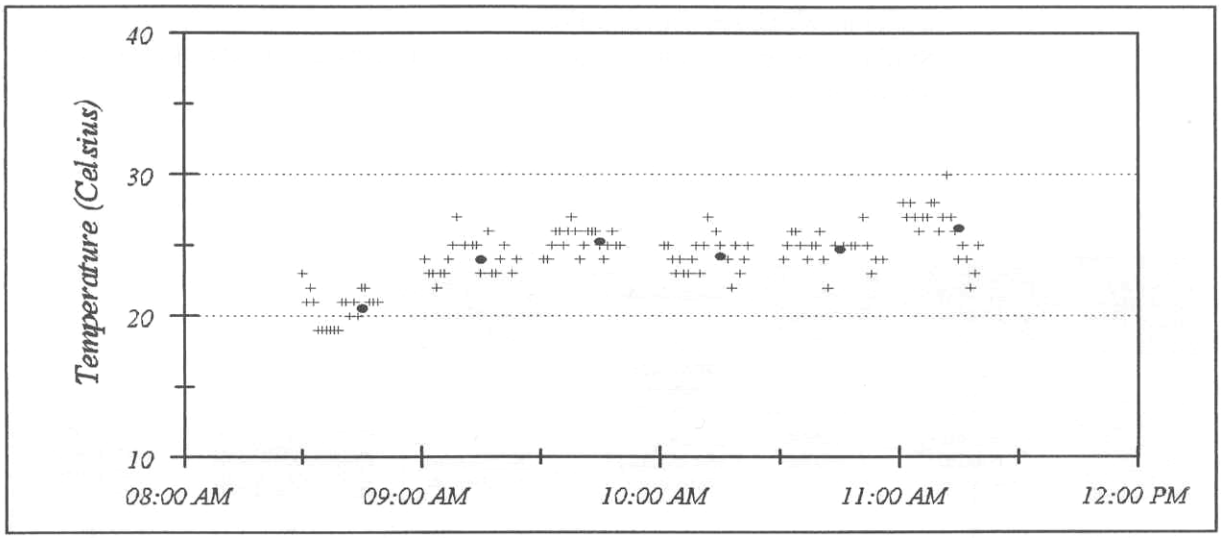

Figure 7. Thermal infrared surface temperatures for the AI Garf site as measured on 13 of May 2000 by a hand-held radiometer. Solid points indicate averaged temperatures per half hour intervals.

Depending on surface conditions, the surface temperature increased during the morning. It ranged from around 20° Celsius around 08.45 A.M. to 26 ° Celsius around 11:15 A.M.. To obtain site specific surface thermal radiation, necessary to perform the atmospheric correction on the thermal satellite imagery , the temperatures were corrected for their wavelength region, emissivity and after that integrated. This yielded a surface temperature of 24.65 °C during the satellite overpass in this case.

2.3.2.3 Meteorological data

For a good implementation of the SEBAL method the following data is desired

- Monthly meteorological data for the years 1989 till 2000 on:
    - Air temperature (minimax)
    - Pan evaporation
    - Incoming solar radiation (airport)

- Daily meteorological data for the following of the satellite overpasses used:
    - Air temperature (minimax) -Relative humidity
    - Barometric pressure
    - Sunshine hours
    - Pan evaporation
    - Precipitation
    - Visibility (airport)
    - Incoming solar radiation (airport)
    - Windspeed

Certain measurements are not available (e.g., pan evaporation), others have no full record and are restricted to the station at the airport.

For SEBAL processing the following data is absolutely necessary (and obtained in the project)

- -Continuous atmospheric data concerning incoming shortwave radiation (data logger at WEC, see above section).
- -Surface temperatures at a representative site during satellite overpasses (see above section).

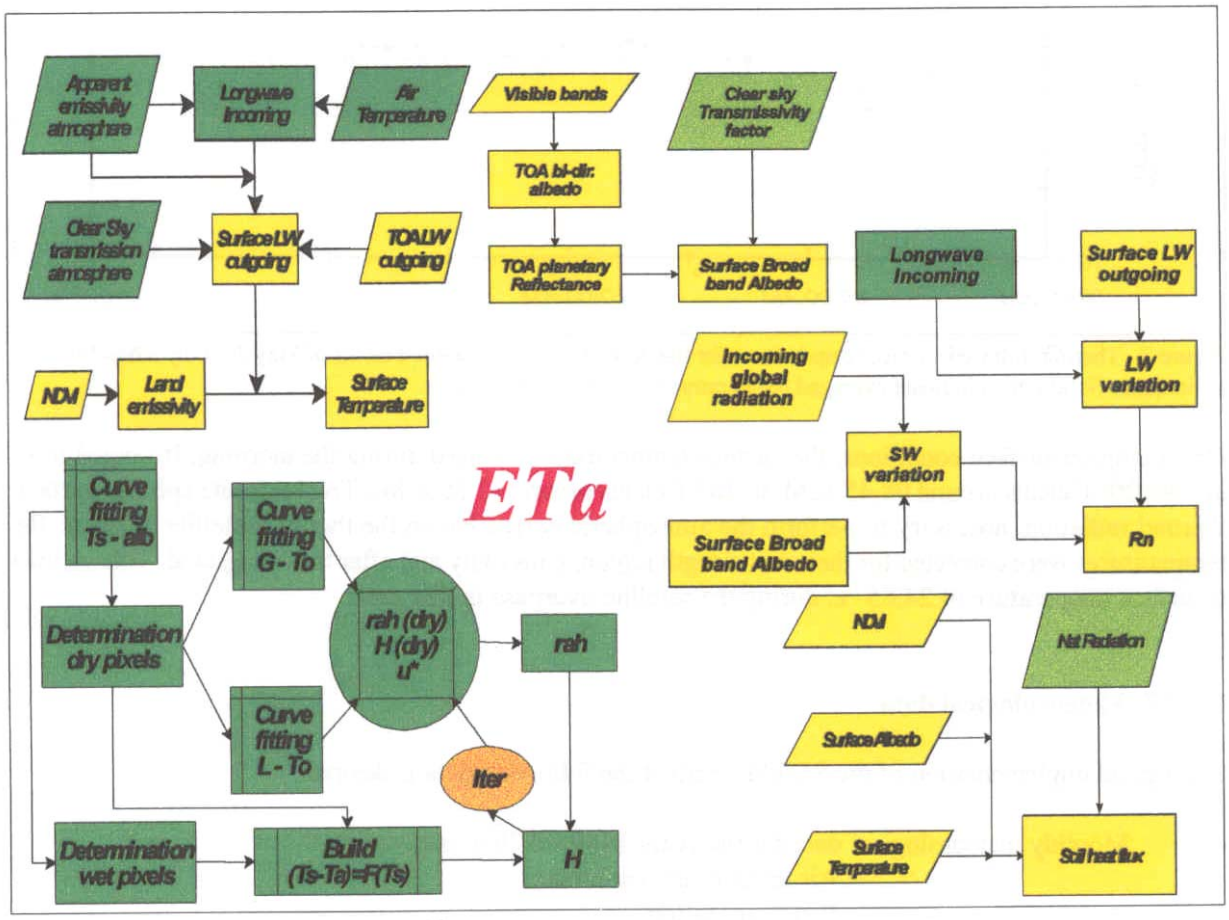

Figure 8. Overview of the SEBAL algorithms.

2.3.2.4 SEBAL processing

The brief description of the method given above, may give a false impression of the complexity of the method, which involves more than 30 calculation steps and many functions.

For an illustration of the complexity of the method, the diagram of figure 8 is included. The SEBAL method was implemented in a combined GIS-RS system (IL WIS of ITC)

2.4 Total water use

When for the entire basin the cropped areas and irrigated areas are determined, and the actual evapotranspiration values for each pixel, by "crossing" (or logical combination or overlaying in GIS- terms) the water use per crop and the totals can be calculated for the overpasses, see Paragraph 3.3.

For the periods between overpasses, use is made in this study because of lack of metereologic data, of the monthly crop reference evapotranspiration using a method based on temperature data and extra terrestrial radiation (Hargreaves method).

Generally, when interpolating between satellite overpasses, or image availability , use is made of some kind of modelling (Farah and Bastiaanssen, 2001). This type of modelling requires daily meteorological input, such as air temperature, relative humidity, barometric pressure, sunshine hours, pan evaporation, precipitation, solar radiation, windspeed, etc. Unfortunately, see the Appendices, there was only I meteostation providing data, and moreover, mostly only historical, monthly data was available from this station (airport). No daily data, except for the days of overpass, could be obtained. The only continuous recording station in the area was the pyranometer installed at the WEC, registering incoming solar radiation. This alone, however, is by far in-sufficient to estimate evapotranspiration rates.
The so-called Hargreaves method (ref. FAO guide, page 64) makes use of temperature (miD, max and average) and solar radiation to estimate crop reference evapotranspiration, see Paragraph 4.1. This method is used here on long-term average meteo data, where the idea is that using the Hargreaves method, a monthly (Long-term average D crop reference evapotranspiration can be determined.

This method is used here in two different ways.

2.4.1 Yearly water use, lumped.

First of all the Hargreaves method is used to derive long-term monthly crop reference evapotranspiration. As a next step the average actual evapotranspiration rates for the main crops (Qat, Grape and other) as determined by the RS algorithms are calculated for the three dates of overpass, assuming that the day the image is taken is representative for that particular month. The ratios of these rates with respect to the monthly values obtained from the Hargreaves method are then used to come to arrive at a yearly estimate of actual evapotranspiration.
In this way, also crude estimates of monthly water use can be obtained, see Paragraph 3.4.1. for the results. However, one has to keep in mind that this is the amount of water consumed by the crops; hence no correction for irrigation efficiency is applied yet.

2.4.2 2.4.2. Yearly water use, spatially distributed.

The second method also makes use of the derived long-term monthly crop reference evapotranspiration rates. Again the assumption is made that the image is taken as representative for that particular month. Note: In general this will cause an over-estimation since an image is typically taken at a cloud-free day, hence the ETa rates for that day will be higher than on a cloudy day.
In this method the ratio of all the pixels in the entire image with respect to the crop-reference rate are taken and used for temporal, monthly, integration. The ratios found from the three images are used for the early season (January till March), the mid season (April till September) and late season (October till December) respectively. After adjusting for the monthly crop reference rates they are summed to provide the yearly totals, see Paragraph 3.4.2. for the results.

This method has the advantage that it is possible to visualize the spatial distribution, which is provided in the map "Crop water use". In addition, the results can be repeated by crossing with subcatchments, to yield figures for the subcatchments for crop acreage, irrigated acreage (very much the same in Sana'a Basin) and actual yearly water use.
They are provided in paragraph 3.4.

3. RESULTS

3.1 Crop types

3.1.1 Crop type pattern

Overview map

- A map at I: 100,000 scale is prepared with the results of the crop classification for May 2000, Plate I. (This map has a large size and is delivered separately, but can also be viewed on a computer).

The background of the map is a satellite image, for more accurate positional reference, as well as land types (young volcanic terrain, limestone area, etc.). Roads and names have been added.

Inspection of the map will learn that not many land cover classes can be shown because of the small sizes of the fields. Therefore, one pixel or clusters of a few pixels only occur in many parts of the basin and they are difficult to observe visually on this scale.

Map with detailed crop types

- The results of the classification for the central part of the basin is shown in Plate II in another scale using various colours, so that small fields can also be distinguished.

3.1.2 Statistics

The statistics for the Sana'a basin are following:

Subcatchment	Total area (ha)	Irrigated area (ha)	Qat	Grapes	Mixed cereals & others	Fruit trees
Alluvium-North	30546	5561	2300	2531	720	10
Alluvium-South	17546	1081	556	240	230	55
Bawsan al Madini	24185	663	198	409	56	0
Darwean al Ghayl	40565	3181	1555	939	642	45
Dula' Hamdan Bani Hawat	6221	774	495	86	157	36
W. al Furs Rijam	5121	1198	659	478	59	2
W. al Kharid***	17913	659	83	568	8	0
W. al Qatab al Ma'adi	11156	187	128	8	45	5
W. As Sirr	22703	3461	1566	1769	122	4
W. Ghaber al I'shash	7260	314	134	52	83	45
W. Hard al Ghayl Zahr	36638	2387	1191	338	732	126
W. Hizyaz Ghayman	36127	893	323	276	251	43
W. Lafaf Asir	20963	1108	908	10	178	13
W. Sa'wan ar Rawnah	8966	870	453	250	154	13
W. Shahik al Ajbar Sha'b	21787	650	251	167	192	40
W. Thumah al Mahajir Shira	8110	393	280	35	70	8
Total	30546	23380	11080	8156	3699	445

Table 1. Subcatchment statistics on ground cover classes. Please note that, as stated on page 37 as well, that a special remark has to be made with respect to Wadi al Kharid. "In the northern part the crop type is classified as grape mainly, whereas fieldwork conducted in the wadi indicated a presence of mainly mixed cereals and vegetables fields, surrounded by incidental fi11it trees. However, no fieldwork was possible north of the UTM- Y 2732400 due to in-accessability. The inaccuracy due to spectral response (soil background?) Affects the crop statistics only, not the statistics about irrigation acreage nor evapotranspiration.

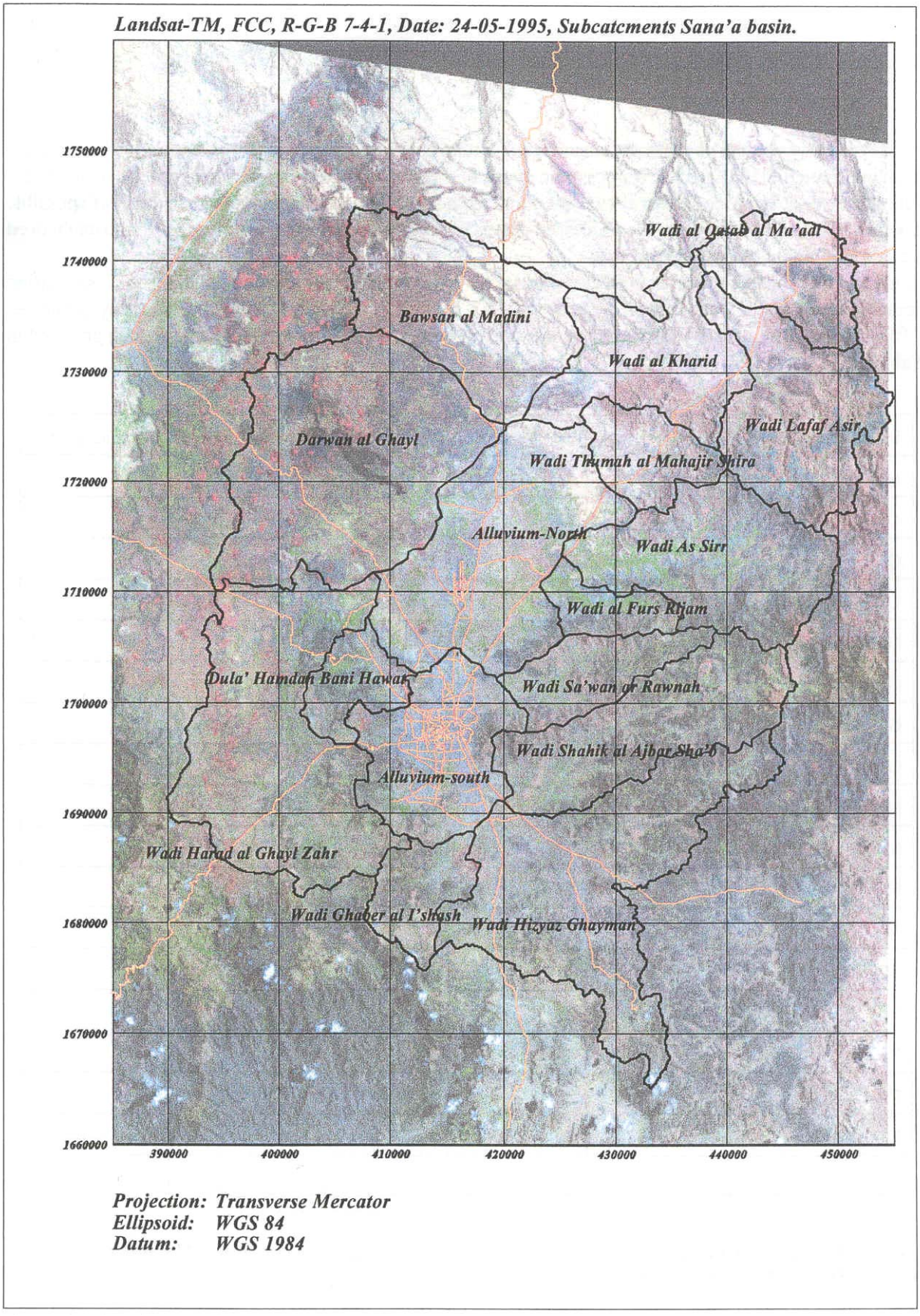

Figure 9. Subcatchments of Sana'a basin.

Please note that no map showing the accurate subcatchment boundaries was at our disposal. Therefore the team interpreted I :50,000 scale topographic maps, combined with field experience in order to come to the subcatchment delineation shown above. We admit there might be some minor inconsistencies with possible existing boundaries. However, the processed data is digital available meaning that anyone who might need a correction could easily perform this.
Using an independent data set as collected during the field campaigns the accuracy of the crop classification could be determined, as described in Paragraph 2.1.1.. The results range from 93% accuracy for grape, 87% accuracy for qat, 81% for mixed cereals and other to 53% for fruit trees. The results are provided in Table 2.

Independent ground truth set	Nr. of pixels	Classified as	Nr. of pixels	Accuracy (%)
Q	247	Q	214	87
Q	247	G	6	
Q	247	M	16	
Q	247	U	11	
G	205	Q	10	
G	205	G	191	93
G	205	M	3	
G	205	U	1	
M	179	Q	1	
M	179	G	7	
M	179	M	145	81
M	179	F	7	
M	179	U	19	
F	38	Q	3	
F	38	G	1	
F	38	M	9	
F	38	F	20	53
F	38	U	5	

Table 2. Contingency table, showing accuracy of the crop classification. Note: Q = Qat, G = Grapes, M = Mixed cereals and other, F = Fruit trees, U = Unclassified.

An overview of the sub catchment locations is provided in Figure 9.

3.2 IRRIGATED AREAS

3.2.1 Statistics and overview maps

The explanation concerning difference between satellite based statistics and field census data in section 1.2.2 should be remembered; *field census data always gives higher values,* because the entire parcel or ownership is used, ir-regardless whether the parcel is fully covered by irrigated crops or not. The satellite data gives a true presentation of the actual situation because it is based on physical measurement of presence of green crops.

Therefore the acreage for the early part of the growing season is lower than for the later part.

Date	Irrigated area (ha)
09-03-1985	9700
12-05-1985	11900
06-10-1989	14700
12-10-1994	23200
16-01-1995	17100
24-05-1995	26800
01-06-1998	27400
26-03-2000	18400
13-05-2000	23400
12-10-2000	27800

Table 3. Irrigated acreage historical development.

The data presented in Table 3 is corrected for mixed pixels (see Paragraph 2.2.2) and shows the historical data.

3.2.2 Overview map of irrigated area

For the sake of convenience and overview, in this report a small scale NDVI map is included in Part II, Figure 13.

The large size map 1: 100,000 with the crop type classes also shows the irrigated areas, because of green fields are mostly irrigated.

3.3 Actual Evapotranspiration

As explained earlier, the total amount of water that is evapotranspired for the days of the satellite overpasses can be determined using the SEBAL algorithms. When applied this gives the following totals for the water use in the basin:

Date: 26-03-2000 Water use: 243300 (m^3 per day)
Date: 13-05-2000 Water use: 210200 (m^3 per day)
Date: 1 2-10-2000 Water use: 112200 (m^3 per day)

And, once again, these numbers comprise the amount of water transpired by the crops, hence they are nett figures. To obtain the amount of water pumped they should be corrected for the irrigation efficiency!

The subcatchrnent totals are provided in the appendices, where also the historical values are presented. However, as stated before, the historical values have to be considered with some caution because not all necessary meteorological data was available and no atmospheric corrections could be applied.

For example, the water use for June 1985 is fairly high. It is not known whether rainfall contributed to this amount, or not.

When the ETa values for cropped areas are summed up, the yearly maximum water use is estimated as between 60.5 and 75.1 million mJ for the year 2000.

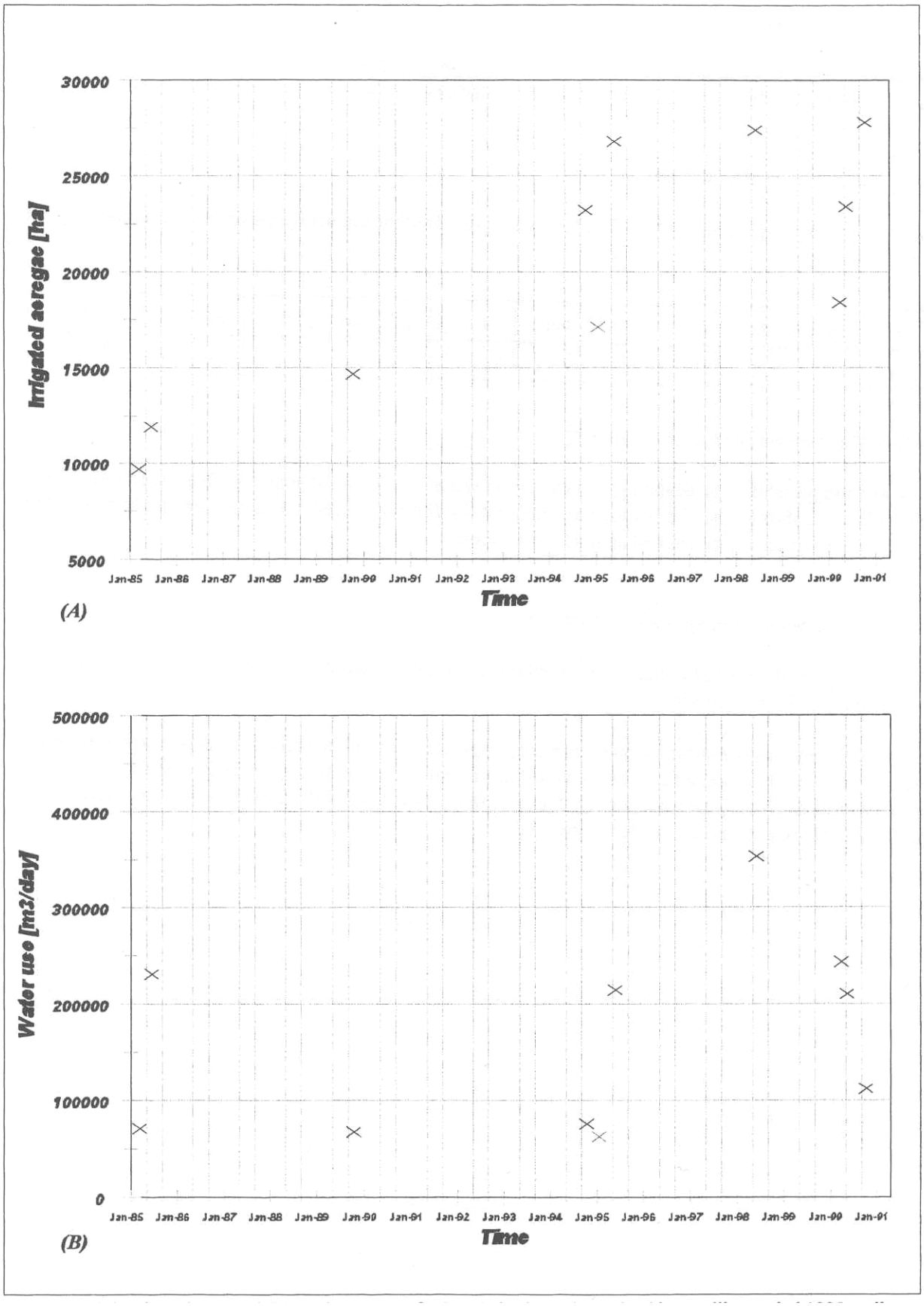

Figure 10. (A) Irrigated area and (B) total water use for Sana'a basin as determined by satellite, period 1985 until 2000.

3.4 Total water use.

As already stated many times before, the totals that are presented here are nett figures. To obtain the gross figures they have to be corrected for the irrigation efficiency (which was not part of the TOR).

3.4.1 Yearly water use, lumped.

When using the Hargreaves method for determining the monthly and yearly water use, the lumped figures are as follows:

Jan	*Feb*	*Mar*	*Apr*	*May*	*Jun*	*Jul*	*Aug*	*Sep*	*Oct*	*Nov*	*Dec*	*Year*
4.2	4.6	5.0	4.5	5.8	6.0	6.0	5.9	5.5	4.7	4.3	3.5	-
5.1	6.2	6.5	6.6	7.2	7.5	7.3	7.2	6.8	5.9	4.9	4.9	75.1

Table 4. The monthly figures in the first row indicate the crop ET values used for the water use estimates and is given in average mm/day. The monthly figures in the second row are the total monthly water use estimates in million m^3.

This method gives slightly deviating values for the water uses than the spatially distributed one. This is basically due to the fact that the evapotranspiration ratios for the different crops with respect to the monthly crop reference rates are calculated as a yearly average.

3.4.2 Yearly water use, spatially distributed.

When applying the spatially distributed method, the yearly amount sums up to 60.5 million m^3.
The yearly numbers per sub-catchment per crop-type are provided in Table 5. To derive seasonal figures technically would be possible, but this would mean that for example for the early season, the estimate would be based on one single image, which would be too daring to our opinion.

Subcatchment	Irrigated area (ha)	Water use (* 100 m^3)				
		Sub-catchment	Qat	Grapes	Mixed cereals & others	Fruit trees
Alluvium-North	5561	90779	44696	33708	12202	173
Alluvium-South	1081	21832	14287	2228	3088	2229
Bawsan al Madini	663	6152	1513	4025	614	0
Darwean al Ghayl	3181	60094	32398	14268	12420	1008
Dula' Hamdan Bani Hawat	774	28309	21811	1319	3611	1568
W. al Furs Rijam	1198	47483	27623	18297	1468	95
W. al Kharid	659	16846	3547	12897	402	0
W. al Qatab al Ma'adi	187	3168	840	2287	36	5
W. As Sirr	3461	13349	68218	61503	3572	197
W. Ghaber al I'shash	314	5676	2999	620	974	1083
W. Hard al Ghayl Zahr	2387	110279	72490	8476	23376	5937
W. Hizyaz Ghayman	893	10362	4182	2808	2430	942
W. Lafaf Asir	1107	46954	29022	11613	6187	132
W. Sa'wan ar Rawnah	870	10731	5556	2568	2104	503
W. Shahik al Ajbar Sha'b	650	5365	1976	1014	1530	845
W. Thumah al Mahajir Shira	391	8000	4210	3363	427	0
Total	23377	605520	335368	180994	74441	14717

Table 5. Subcatchrnent statistics on water use per ground cover class.

An overview of the irrigated areas by crop type and their respective water use is provided in Table 6.

Crop-type	Acreage (ha)	% of total	Water use (10^6 / year)	% of total
Qat	10300	44.1	33.5	55.4
Grapes	9130	39.1	18.1	29.9
Mixed cereals and other	3530	15.1	7.4	12.2
Fruit trees	420	1.8	1.5	2.5
Total	23380	100.0	60.5	100.0

Table 6. Crop acreages and water use, total Sana'a basin.

4. Conclusions and discussion of results.

The main findings are given in the executive summary.

4.1 Satellite-based actual evapotranspiration and crop reference evapotranspiration

Satellite-based actual evapotranspiration

The actual evapotranspiration values for the three overpasses during the year 2000 have values which range from 2 to 5.5 , with a few fields with slightly higher values.
For the year 2000 no cloud free images were recorded during the main development of qat and grapes (June-September). The Eta calculated for June in two earlier years, showed a notable increase, but no field calibration data was available for those earlier years. This increase can be expected because the crop reference evapotranspiration is high during summer months and the crops are in full leave.
Adjustments were made to include higher Eta values in the months of June -August 2000, for the estimation of the total water use.

The spatial distribution pattern of Eta for the overpasses could be well established.
This study shows important spatial variations in the kc factors, due to variations in crop and irrigation management, soil conditions, density of the crops and so on (see section 4.4.)

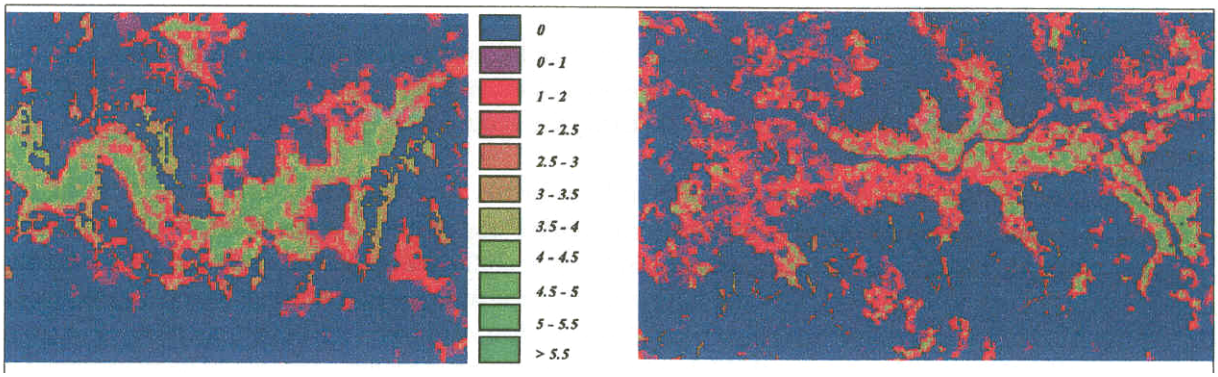

Figure 11. Evapotranspiration results for part of Wadi Dhar (A) and part ofWadi As Sirr, date 13-05-2000.

However, when this pattern is studied in detail, a large number of single pixels or small clusters of a few pixels are found where the Eta values are below 3 mm.d-1. on all images for which Eta was calculated. Figure 11 of Wadi Dahr and Wadi As Sirr also contains such areas. Possibly these small areas are receiving little water from shallow wells. Some of the small fields could be rainfed crops, as discussed a marginal effect only. An extensive field survey is required to determine the relation between irrigation management and the lower limit of Eta of irrigated crops.
The study itself and the evaluation of the results are severely hampered by lack of meteorologic data, due to a time gap between measurement at the airport and release.

Crop reference evapotranspiration

Results of the satellite based actual evapotranspiration should be compared to the crop reference evapotranspiration.

The new guidelines (Allen at el. 1998, F AO) facilitate the calculation of the Penman-Monteith (P-M) equation using generally available meteorological data. That equation is now generally accepted as the best standard. However, implicitly, it is assumed that the meteorologic parameters required for the calculation are derived from a station situated on a large grassland with a surface resistance of 70 s/m. (i.e. well watered conditions.). The set of parameters, available only for a very few years, are derived from the airport of Sana'a City, where the conditions are much drier than those for the crop reference conditions. Therefore, the values

calculated with the airport data will be too high, particularly in the summer months. For the year 1998, the P-M method resulted in monthly ETO ranging from 3.43 mm.d-1 in December to 8.42 mm.d-1 in July. The latter value is therefore doubtful.
The Hargreaves method offers an alternative, since only temperature data and extraterrestrial radiation is required. However, this data is available for the historical period of the study, excluding 1994 and 1995, only.
The results of the Hargreaves method, ETOHargr.. varies from about 3.9 in December to about 6 mm.d-1 in July during the period 1989-1999. The appendix shows a comparison between the two methods.
However, the simpler type of equations, such as the Hargreaves equation, assumes a wind speed of 2 m. S^{-1}. Wind speeds from the airport for the summer months are more than that, and the Hargreaves value may be on the low side.
Therefore the ETO in the summer months will be between the Hargreaves and the P-M figures.

4.2 Total amount ofwater used

The determination of the actual evapotranspiration (Eta) for the year 2000 results in between 60.5 and 75.1 million m3. in the entire Sana'a Basin. The way this was calculated is explained in Paragraph 2.4. the real use will be in a range around these figures, considering the accuracy of determination.

For the estimate of the total water use, the Eta values for the irrigated crops have been summed up. However, it is possible that due to classification error rainfed crops have been classified as irrigated crops. The Eta values for the three dates of overpasses in the year 2000 showed some variation, which needed examination. Usually the variation is influenced by rainfall and atmospheric evaporative conditions in the days prior to the overpass. For example, rainfall one or two days prior to overpass causes a general increase in soil moisture and consequently higher Eta values during overpass. This might be an explanation for the slightly higher total of March over May, Paragraph 3.3. However, no preceding meteorologic data could be obtained to study the causes of the variation.

The major difference is seen with respect to the October image, where the total water use is at about 50% of those during March and May. As stated before, the evapotranspiration rates are influenced by meteorological conditions. In the October image the average day temperature was 17.2° Celsius, whereas for the other images the average day temperature was 22.4° and 22.7° Celsius respectively. It is known that this influences the amount of transpired water considerably.

Another problem for arriving at a total figure for Eta over a full growing season lies in the estimation of the actual evapotranspiration between satellite overpasses. Because only continuous average temperature data was available, the method of Hargreaves (included in the FAO Guide lines) was used for the calculation of the crop reference evapotranspiration (ETO), for this purpose.

Therefore, the total water use, as calculated, should be regarded as "best estimate", and it is not likely that it is an underestimate. For example, when taking into account of 40% *irrigation efficiency we arrive at a total of in between* 150 *and* 190 *million* M. *Comparing this figure to a groundwater modelling study (Foppen,* 1996) *a similar value* (182 *million* M) *was assumed. However, with small scale groundwater irrigation the efficiency might be higher.*

4.3 Accuracies

In the sections where the methods are explained, attention is given to:

- The difference between census data based on field surveys or cadastral data and data obtained
- by remote sensing.
- The problem of the mixed pixels because of the small sizes of many fields or parcels in relation to the spatial resolution of Landsat TM. However, after aggregating the individual small parcels into the class "Mixed cereals and other" this problem is mostly solved.

Despite a careful approach and correction to account for the above problems, the figures presented in the tables in section II, and in the executive summary, should be regarded as values, which fall within a certain accuracy range.

Crop types
The crop type classification, when tested with an independent sample set, is within acceptable limits. It varies from 53 to 93% accuracy, depending on crop type.
The standard method of assessment, although applied, does not honour the problem with the mixed pixels. Hence, the accuracy could be a little better, or a little worse than indicated
Multi spectral classification using the high resolution IKONOS data (4 meter resolution!) could give more accurate results, but at a high cost.
An IKONOS study could for example be tested on a small area. The costs involved are US$ 29 per square km. Images for the study area are archived at the Dubai receiving station for the 2000 summer period. A minimum area should be purchased of II xll km, delivery time approximately 4 weeks. It is also possible to have the satellite programmed for future acquisition of images over the area.

A special remark has to be made with regard to Wadi AI Kharid. In the northern part the crop type is classified as grape mainly, whereas fieldwork conducted in the wadi indicated a presence of mainly mixed cereals and vegetables fields, surrounded by incidental fruit trees. However, no field work was possible north of the UTM- Y 2732400 due to in-accessability .The inaccuracy due to spectral response (soil background?) Affects the crop statistics only, not the statistics about irrigation acreage nor evapotranspiration.

Actual evapotranspiration
In the Sana'a Basin, the accuracy of the Eta data obtained by satellite can only be assessed by large Iysimeter tests or by careful field experimentation with known water application and measurement of soil moisture transport within and below the root zone.
Such test should be carried out over a range of soil, management and crop stage conditions, found in the Basin. Furthermore, wind speeds in the valleys surrounded by high cliffs will be different from those in the open alluvial area north of Sana'a city .It is well known that wind speed has much influence on evapotranspiration. However, none of such field test results is available.

It should be noted that the mixed pixel problem does arise in the calculation of Eta, because a partial cover of crops within a field or a pixel results in different temperatures registered by the satellite sensors.
As will be discussed below, the Eta/ETO provides a crude check on the results. Generally it is expected that for grapes ETa/ETO < I. This is indeed the case, confirming that the satellite based figures are realistic.

There are some pixels where the ratio > 1, but this is expected because there are trees in the grape and qat areas. Aerodynamic resistance is less pixels with trees and their roots make use of irrigation water. furthen11ore, when soil of a field is very wet, just after irrigation, ETa/ETO = 1.1 (f AO Guidelines, 1998).

Sensitivity analysis
Surface flux densities and moisture indicators obtained by applying the 36-step SEBAL procedure comprise deficiencies and failures on (i) radiometer calibration, (ii) atmospheric correction, (iii) empirical relationships, (iv) spatial variability of hydro-meteorological parameters (v) simplified energy budgets, etc. The various model parameters of SEBAL are, without exception, all directly or indirectly estimated from spectral radiances and therefore associated with more or less uncertainty and results should be termed 'estimations'. The effects of the parameter variability on these estimations are addressed here by describing their sensitivity: A numerical estimation of the first derivative of a certain model parameter on a certain output parameter. All relevant model parameters were considered one by one, while keeping the other parameters constant according to the values for the reference situation. The relative importance of each independent model parameter on the surface flux densities and moisture indicators appear from this analysis. The discussion of the model output here is restricted to the latent heat flux (and thus the actual evapotranspiration) only.

Input, x_i	Description	Fractional difference					
		Irrigated part		Dry part		Aggregated	
r_0	Surface albedo	-3.8	5.7	-91.0	-13.3	7.4	-8.6
$K^{\downarrow}$	Incoming shortwave radiation	23.8	-20.0	-85.7	-97.1	17.4	-22.9
$L^{\downarrow}$	Incoming longwave radiation	15.2	-10.5	-12.4	-32.4	6.9	-7.2
ε_0	Surface emissivity	1.9	-7.6	-59.0	-58.1	-4.6	-7.5
T_0	Surface temperature	-10.5	14.3	-77.1	24.8	-8.6	5.3
Γ	Soil heat flux/Net radiation ratio	-2.9	2.9	-25.7	-96.2	-3.2	-2.4
z_{0m}	Surface roughness length	0.0	0.0	0.0	0.0	-2.6	1.1
kB^{-1}	Roughness for momentum/heat flux ratio	1.9	-1.9	-1.0	5.7	0.9	-2.9
u_*	Friction velocity	0.9	0.0	1.0	0.0	0.7	-1.3
$\delta T_{a\text{-}ra}$	Near-surface vertical air temperature difference	1.9	3.8	-37.1	102.0	-3.3	7.8
NDVI	Normalised difference vegetation index	5.7	-1.9	-82.9	-30.5	-10.1	3.8

Table 7. Results of the sensitivity analysis for *the SEBAL algorithm.*

SEBAL uses 12 hydro-meteorological input parameters, of which 10 are independent. Although the NDVI is not a direct hydro-meteorological parameter in the SEBAL procedure it is included in the sensitivity analysis to provide a better understanding. The sensitivity analysis is based on a fixed 25% change in the 11 model parameters, Xi, (Table 7) with respect to their values of the standard run, while keeping all other parameters fixed. As may be clear from the description of the SEBAL algorithm it matters whether the method is applied over homogeneous or heterogeneous terrain. In general the method improves when applied over heterogeneous terrain. This is also clear from the results presented in Table 7, where the relative sensitivities are illustrated as fractional differences: (AE-AEref)/AEref. The analysis is performed over homogeneous irrigated areas, homogeneous dry areas and over aggregated areas. The results of the fixed 25% increase of Xi are shown first, where-after for the same Xi the results of a 25% decrease are presented. The results show that for the irrigated areas, the latent heat flux is fairly in-sensitive for all variables, whereas for dry areas relatively large fractional differences are seen. However, in our case the interest lies in the crops, which show fairly good results. Furthermore, the incoming solar radiation is recognized to be a sensitive parameter for Eta determination, which is known from literature as well. As stated before, the aggregated areas show fairly stable responses, where again the incoming solar radiation appears the most sensitive parameter. In general it can be stated that the actual evapotranspiration rates can be accurately estimated over relatively wet and/or heterogeneous areas, whereas over dry and homogeneous areas it is recommended that alternative procedures are investigated.

Irrigated areas
For the irrigated area it is difficult to give accuracy limits because of the comparison problem with census data (see section 2.2.2.). In any case, no proper census data is available.
In our opinion, the satellite approach is preferred if the water balance is of interest, as is the case. In case of land tenure or taxation purposes, the parcel approach would be of interest.

Historical data derived by satellite
For the historical data it is not possible to assess the accuracy of the crop types, because no independent data set is available. The training set collected for the year 2000, complemented with the data set for accuracy assessment in the same year, could be used for grapes and qat because these crops have long lifetimes.
Reviewing the historical trend in irrigated acreage since 1985 (the flfSt image used) shows an increase, which seems to stabilize after 1995. The increase prior to that period is in line with statistics showing the increase in number of drilled wells in the period up to 1995 (Foppen, 1996).
With respect to the seasonal variation, the statements made in Paragraph 2.2.2. concerning dense crops might be remembered. The satellite data gives a true presentation of the actual situation because it is based on physical measurement of presence of green crops. Therefore, in general, the acreage for the early part of the

season is lower than for the later part. In general, the acreage under irrigation is low in winter (January images) and starts developing to its maximum around July (middle of grape season), whereas it goes down until the end of the season. Normally in October still higher values are observed than in mid winter. In addition, it should be noted that the grape season spans roughly from May/June till September/October. Most probably the high June 1998 result just covers the start of the grape season, whereas the May 2000 image just missed it. ,

4.4 Derivation of and comparison with kc factors

A much used method to estimate the crop water use under good management conditions, is often done by using kc factors. The kc factor, defined as ETa = kc. ETO (Allen et al.,f *AO,* 1998) where ETO is the crop reference evapotranspiration. The new guidelines (Allen et al. 1998, f *AO)* contains rules to separate soil evaporation with crop transpiration (dual factors) and take account of stress conditions. Considering the large variation in satellite-based Eta noted, future field studies should attempt the use of the dual crop factor and include stress conditions. By doing so a range of kc values will result, depending on irrigation and management practice. The kc tables in the f AO Guidelines are intended to work out water requirements under good management conditions. Therefore, the satellite based kc factors were worked out in selected areas with good productivity (Wadi As Sirr, Wadi Dahr, etc.) and by looking at values > 3.5 mm.d^{-1}.
For grapes and qat the kc factors based on the May 2000 image work out to be in the range of 0.45 to 0.9. The generalized, single kc factor, according to the tables in the f AO guideline for grapes in mid season is 0.85. for May, it could be a little lower. The satellite based data center around that averaged kc value. The kc factor for the initial period (e.g. March 2000) is too variable for strict comparison, because of the soil moisture status and -unavailable rainfall data at this stage.
Unfortunately, no kc factors for qat are listed in the FAO table, probably because no reliable data was available. The satellite data suggests that there is not too much difference in kc factors between qat and grapes for the areas with good productivity (Eta > 3.5 mrn. d^{-l}).

5. RECOMMENDATIONS

Studies of this nature require the availability of meteorological data, of which incoming radiation is of prime importance, next to the other parameters required to calculate daily Penman-Monteith crop reference evapotranspiration (ETO).

Data from a well maintained and installed evaporation pan would also be welcome, mainly as a back up in case of failure of meteorologic instruments.

Timely access to the meteorological data .is important if satell.ite data is to be used.

For the year 2000 only three cloud free images covering the cropping cycle were available. (The first two were Landsat 7, the one for October, was Landsat 5 obtained from the Dubai rece.iv.ing stat.ion, on Thursday 251h of January!). Availabil.ity of more images will improve the accuracy of the determination of the amount of water used by crops (irrigation drafts). The new generation satellites with multispectral and thermal sensors (ASTER, MODIS) will soon offer, in conjunction with Landsat, an increase in temporal coverage.

Hence an effective monitoring of the groundwater use by irrigation is possible with reasonable accuracy by a combination of satellite data and standard meteorological data (first order station). In case future studies in Yemen (e.g. Taiz, Hadhramaut, etc.) are planned, this point should be considered. ~, To obta.in a better knowledge of the crop water use, the data presented in this study provides a basis.

Improvement in the accuracy of crop types and irrigated acreage can be achieved by using high-resolution multi spectral images, such as IKONOS data. The problem of mixed pixels will be minimized. However, acquisition of that type of data is still expensive. B

This study might be combined with a more extensive research after the vegetation types and land cover in the basin. This should be combined with a more extensive fieldwork, using multi-spectral radiometers. Parallel to this an effort should be made to improve the accuracy of the distinction between irrigated crops and rainfed crops, especially in the southern part of the basin, where this is practice. Once again, local farmers should be interviewed, but more important; sufficient daily meteorological data should be made available.

Recently, an improved method for assessing ETa in between satellite overpasses and cloudy days, is based on the use of the Penman-Monteith and Jarvis-Steward models was researched and published (Farah & Bastiaanssen, 2000), but the method requires parameter values (surface resistance) which are difficult to obtain. However, they also found that the method of the evaporative fraction (used in this study to obtain daily values) could be used to cover periods of a week. This entails a less data demanding simplification. For testing this application the Bowen ratio should be determined over the crops in various parts in the Sana'a Basin by installing small towers in irrigated fields with temperature and relative humidity sensors, complemented with a pyronometer.

PART II HYDROGEOLOGICAL INTERPRETATION OF SATELLITE IMAGES

6. Hydrogeological significance of the map showing relative recharge and lineaments.

6.1 Introduction

Remotely sensed images have been used for three purposes:
a. Study of lineaments
b. Mapping units of relative recharge
c. Study of the distribution of areas, irrigated by groundwater.

a. Lineaments

A well known application of satellite images in hydrogeology is the study of lineaments, which are associated with faults, fractures and large master joints, depending on the scale of study. These linear features cut across the rocks and create "secondary permeability", in addition to the permeability associated with the primary porosity of the rocks.
The small scale of the satellite images (1:500,000 to 1 :50,000 maximum) allow the interpretation of the major lineaments. On a -small- scale of 1:500,000 the larger and therefore often more deeper structures are seen. On aerial photographs, which show only a small part of a region, large master joints can be observed.

In well tests carried out in the Sana'a basin it was shown earlier that high permeability or transmissivity were, in each hydro-lithologic unit, associated with fracturing. Many studies in the literature have shown that well yields can be related to proximity to lineaments. However, not an interpreted lineaments are open fractures or faults carrying groundwater.

Through the main lineaments subregional groundwater flow may occur, depending on overall head conditions. This could mean either a loss or gain of groundwater in a given aquifer.

The mapping of lineaments is essentially based on visual interpretation, which can be done on good quality hard copies of remote sensing images, or can be done on the computer screen.
Preprocessing of the digital images requires only standard image processing programmes, such as filtering and preparation of colour composites, but also study of individual images resulting from orthogonal decomposition (such as the Principal Component Transform) may be done.

Since the operations are not too time consuming, the study of lineaments is recommended as a standard practice. It would be worthwhile to do interpretations in such areas as Taiz, Hadhramaut etc.
In later sections in this report details of the significance and interpretation of lineaments is given and recommendations for further work.

b. Mapping units of relative recharge

The images provide a means of differentiating and delineation of terrain units which describe qualitatively the relative recharge. This is based on combination of the type materials found near the surface (alluvium, colluvium, rock outcrops) and the relative runoff intensity as a function of slope steepness and depression storage. The lower the runoff intensity, the higher the probability that water can infiltrate episodically.

c. *Study of the distribution of areas, irrigated by groundwater.*

In the Sana'a basin it can be assumed that the groundwater conditions are more or less reflected by the presence or absence of irrigated fields.
Therefore it is worthwhile to study the pattern of the irrigated fields with the aid of a image, which has been transformed to show the green vegetation. In the summer of the semi arid Sana'a basin, green vegetation is highly associated to irrigation by groundwater.
The pattern of the irrigated fields is compared with some existing geologic data in this study.

6.2 Geologic maps consulted.

The map is based on interpretation of Landsat images. No field studies have been carried out.
Two available geologic maps were intensively consulted to provide ground truth. The maps are:

Geological map Sana'a, sheet 15 G. 1:250 000 , The Natural Resources Project. Ministry of Oil and Mineral Resources, Oil and Mineral Corporation, Mineral Exploration Board, Republic of Yemen. The map was prepared by Robertsen Group Inc. Year of publication is not mentioned on the map. This map is referred to as the "Sheet 15 G ".

Geological Map of the Republic of Yemen, Sheet San'a', 1 :250 000, Ministry of Oil and Mineral Resources, San' a, Republic of Yemen/ Federal Institute for Geosciences and Natural Resources, Hannover, 1991, Federal Republic of Germany. Authors: W. Kruck and U. Schaefer.
This map is referred to as the "map by Kruck".

6.3 Notes about the consulted geologic maps and their differences

Both maps mention that Landsat TM images were used.
Comparing the geologic interpretation by the present author with the contents of the map by Kruck learns that interpretations have much similarity .It thus seems that much of the boundaries, particularly of the valleys (and their alluvium) are based on image contents. The map by Kruck shows a stratigraphic differentiation, which must be based on fieldwork and earlier geologic reports. This map shows, in the area of interest, no "proven faults' .Except in the limestone area in the north, also the line-symbol representmg " fracture, fault, lineament: uncertain" 'has been used very sparingly. In this study not all these lines could be recognized.

Sheet 15 G shows more geologjc detail. However, the Cretaceous rocks have been grouped into one unit "Tawilah Group, undifferentiated", and no Paleocene is recognized (the Medj-Zir sandstone), as is done by Kruck.
In the upstream part of Wadi As Sirr the two maps differ appreciably in the extension of the sandstones; where Kruck shows sandstones, sheet 15 G volcanics. The opposite can be observed west of Wadi Dahr and even just east of Sana'a. We have taken spectral signatures to make a choice between the two and added a question mark to our map. In some cases of contrasting map evidence, Foppen (pers. comm.) could clarify the issue.

The sheet 15G shows a considerable number of faults and lineaments. Some of the faults could be recognized in the interpretation of the present author, some not, despite the use of image enhancements at different levels of enlargements. If no traces could be found, they have not been included in the interpretation map.

The two geologic maps differ at places much in the delineation of the alluvial areas. Any geological mapping will adopt its own standard for showing alluvium of a certain thickness. Since alluvium of shallow depth occurs at many places, differences in geologic mapping can be expected. Because presence of alluvium is important for recharge, in the study a differentiation of the alluvial areas is attempted.

Also differences were found between the maps and the hydrogeologic reports. For example, for the groundwater modelling, Foppen (1996) prepared a map of the thickness for the Cretaceous sandstones (SA WAS Tech. Report no.05, Volume II: Data availability, figure 3.5). He shows wedging out of the sandstones (which are overlaying the Jurassic limestones) in the area NE of the airport (around and south of UTM latitude 1720000- road Sana'a-Marib). In another figure (4.9) Foppen shows head decline in boreholes in the sandstones, at latitude UTM 1719000, giving credibility to his views.
Sheet 15G shows limestone outcrops in the same area. The mu1tispectral signature in that area is similar (but not precisely the same) to that of the Jurassic limestones. The map of Kruck shows alluvium, but the topographic background information indicates here and there "rocks". In this case the issue was resolved classifying the area as " thin alluvium over limestones/sandstones".

7. Hydrogeomorphological units and relative recharge.

Estimation of the relative recharge is based on depth of water during episodic runoff events, depression storage and presence of channels or alluvium, slope of the terrain and the nature of the deposits. It is assumed that during years with "normal" rainfall, little or no recharge will take place, because the potential evapotranspiration exceeds by far the rainfall. In other words, the infiltrated water in the upper part of the soil will be lost by evaporation. However, once every so many years much rainfall in short periods may occur. Particularly at places where the water collects in depressions or flat areas, conditions are favourable for recharge because the depth of water can be appreciable as well as the duration of inundation. Bypass flow (i.e. flow through root tunnel and fractures, etc) can be an important component of the overall average annual recharge, which generally is very small in such semi arid regions.
Of importance in the evaluation is the contribution of runoff from outside the unit. This pertains chiefly to the alluvial units in the northern part of the basin and the valley units.

A ranking of the units categories of "relative recharge opportunity" is given at the end of the section. The term "opportunity" is preferred, because the ranking is based on qualitative assessment only.

7.1 The units

A. Recent Wadi alluvium.

For the mapping, it was decided to use the "wadi spreads" as shown on the topographic map 1:100.000 instead of the remote sensing images. This was done because the topographic map contents are based on high quality aerial photographs, which show much more detail than the images.
Highest recharge will take place in this unit because of depth of water, the duration of flow and the permeability of the deposits.

Northern basin alluvium

The multi spectral images show quite some variation of the reflection properties of the surface materials. However, it was difficult to identify their nature by interpretation only. Also, the subsurface conditions will be of interest. Therefore is was decided to differentiate the alluvium on the basis of provenance (i.e. the rock types and topography of the catchments supplying the sediments). The reason for doing so is that the nature of the (subsurface) deposits will be much influenced by the type of materials delivered by the wadis.

As was shown by Selkhozpromexport (1985) the alluvial deposits form a sort of trough with the greatest thickness (225m) around the airport. Subsidence must have taken place, attracting the fluvial deposits. Subsidence at such small scale is usually accompanied by flexuring and faulting. The images were therefore carefully inspected for any traces of such faults of flexures in that area, but no visible evidence was found because they are covered by alluvium.

There are no signs of significant flows leaving the basin to the north. Hence it seems that surface water from the wadis is infiltrated, signifying fairly high permeability .

The subunits differentiated on the map are:

A1 Extension of wadi deposits
This unit pertains to the continuation in the northen alluvial basin of the "wadi spreads" of the larger wadis in the valleys. The deposits are of recent to subrecent age. The delineation is based mainly on the patterns, because the deposits have no unique spectral signature. Episodic flows from the wadis in the hills spread out and infiltrates. Therefore, these units have a high relative recharge. Irrigated areas are found within this unit.

A2 Deposits of sandstone/volcanic provenance
This unit comprises alluvial deposits which are less affected by major flooding and therefore recharge will be less than in unit A1

It is likely that the sand content is higher than units of volcanic provenance.

A3 Deposits of young volcanic provenance
Since no major wadis contribute to the depositional area, it is likely that the superficial deposits consist of sheetwash deposits mainly. The provenance rocks have low quartz contents but rich in ferromagnesian minerals. This could well affect the weathering and permeablity of the deposits. In large parts of this unit few irrigated areas are found

A4 Deposits of the central basin
These alluvial deposits have mixed composition.
Irrigated areas are concentrated east of the airport and in the northern extension.

A5 Thin deposits on sandstones and limestones
No major wadis are found in the provenance area. They consist of colluvium and sheetwash deposits mainly. Quite some irrigated areas are found in this unit, which could point to penetration of wells in the sandstones.

Quaternary volcanic plateau in the north-west
The Quaternary volcanics rocks consist of a wide variety of volcanic rocks (see published geologic maps), of varying permeability.

Vd Basalt terrain, irregular, low topography, high depression storage, isolated small volcanoes Runoff from outcrops will accumulate in the numerous small depressions. During episodic spells with high rainfall, accumulation of water in depression may be so much that recharge to groundwater takes place.

Vb Basalts, relatively smooth terrain, little local alluvium
Recharge conditions are less favourable than in unit Vd

Vs As unit Vb, but with sedimentary or tuff intercalations outcropping Recharge as in unit Vb

VI Subrecent lava flows, high depression storage Recharge as in unit Vd

Vf Basalt flows The flows are older than those of unit VI. Morphology of the flows dominates topography, few elongated narrow valleys in between the lava flows. The valley bottoms support vegetation. It is likely that recharge takes place episodically though the valley bottoms, which comprise only a small percentage of the total area of the unit. Recharge conditions are intermediate between units Vd and Vb

V pi Volcanic plateau
Topography is gently sloping to flat, with the exception of isolated volcanoes and cliffs. Irregular pattern of shallow alluvial deposits.
Because of flat topography and presence of alluvium, little water may leave the unit. Some recharge during episodic heavy rainfall, mainly through the alluvial deposits, fed by overland flow.

Vm Mixed volcanics; volcanoes, flows, plateaux
Recharge will be as low to intermediate (as Vb or Vf)

Units of the older volcanic terrain

The younger volcanics have been differentiated from the older ones of Tertiary age (Basalt, Trachyte, Rhyolite and Ignimbrite and ash flow deposits) because of possible differences in compaction (affecting permeability) and because surface roughness is different.

Ti Valleys and footslopes in mainly ignimbrites and ash flows (Tertiary age mainly) Episodic runoff from surrounding hills

Th Hills in volcanic rocks (Tertiary age mainly))

Because of rapid drainage and absence of soils, no recharge

Units of sedimentary rock terrain

The sandstone areas have been differentiated because they form a productive aquifer and show therefore an association with the irrigated fields. The limestones are shown because fractured groundwater flow can be important, in relation to the lineaments and faults shown in the map. Available evidence of the heads (see F oppen, 1996) shows that the groundwater surface in the northern alluvial basin slopes to the north. It is therefore possible that some water is lost to beyond the basin through the fractures.

S Sandstone outcrops
No differentiation is made between the Medj-Zir and Tawilah sandstones, as is done on the map by Kruck. They have been grouped, as is done on Sheet 15 G. Differences between the maps are noted by (?).
On sloping rock outcrops recharge will be insignificant. Some recharge may take place episodically on the footslopes and colluvium.

L ***Limestone outcrops,***
The outcrops are generally gently sloping.
Recharge is limited to bypass flow in depression areas developed along fractures, with some soil cover. Overall recharge is estimated to be low, except when surface karst (not detectable on images) creates depression storage.

7.2 Ranking of the units according to their relative recharge opportunity.

Units with best to medium recharge opportunities a

A1.

A2, A5

A3, A4, A6, Ti, S, L

Units with medium to poor recharge opportunities Vd, , Vdi, VI

Vd, Vdi, Vl

Vf, V pI, Vm

Vb, Vs

Units with poor recharge oDDortunities

Th

8. Lineaments.

8.1 Hydrologic significance of lineaments

General remarks
Overall permeability is increased by the presence of joints, master joints, fractures, shear zones and normal faults. Next to primary permeability , which is related to porosity of the rocks, the joints- fractures create what is termed as "secondary" permeability .
However, the secondary permeability decreases with depth, particularly over the first tens of meters from the surface. Beyond that depth the smaller tensional features Goints) tend to close because of pressure and little effect of weathering (excluding solution in limestones). For that reason, only the lineaments larger than I to 1.5 km have been selected for presentation on the map.
It is assumed that long lineaments extend to larger depths, i.e. they may reach beyond the groundwater table and thus influence groundwater flow.
It is likely that the lineaments correspond to tensional fractures and faults, because study of available geologic data does not reveal ductile conditions (e.g. upthrusts, compressional tectonics).
In the Sana'a basin, hydrogeologic investigations have shown the large differences in permeability or transmissivity values of, in decreasing order: fault zones, fracture zones and undisturbed rocks, see Foppen (1996).

8.2 Outt1ow through basin margins

North
For the overall water balance of the Sana'a basin, water leaving the basin through the larger fractures and faults should be considered. Such outflow can occur through the fractures if the piezometric heads near the boundaries allow this to happen.
Of course, outflow through the porous matrix of the rocks may also happen, but is not discussed here. In limestone country (northern boundary), it is known that karstic (solution) systems, as irregular tunnels and cavities, may have developed along lineaments, even tough the limestones do not show much surface karst. Karst often develops over long period of time as is associated with -fossil- groundwater levels and flow systems. Therefore, it cannot be excluded that groundwater leaves the Sana'a basin through the sandstones and limestones in the north. This is conditional to the piezometric surface being lowered to the north. The latter seems to be the case. The springs at the head of Wadi al Kharid could bear witness of the outflow, provided the hydrochemistry of the spring waters is similar to that of the groundwater of the alluvium and Tawilah sandstone. The fact that the spring discharges has declined during the period of important groundwater abstraction in the northern Sana'a basin, suggests a hydraulic connection.

Also along the north-eastern boundary groundwater may escape from the basin through the sandstones and perhaps through the underlying limestones. However, it is not known whether -fossil- karst systems occur at greater depths. They could have been developed during the Jurassic- Upper Cretaceous hiatus and at places where thin sandstones overlying limestones occur .

East
Along the eastern and southern boundaries groundwater may flow out of the basin because of topographic conditions. The flow through the upper saturated part will be mainly through fractures because the Tertiary volcanics have low intrinsic permeability .At larger depths flow could occur through the sandstones which crop out beyond the eastern boundary .However, not many major fractures could be identified in that area and fracture flow is therefore supposed to be low.

South
Volcanic rocks make up the area around the southern boundary. Some major fractures and a few normal faults occur in that part. Both geologic maps agree on the existence of a fault just west of the road from Sana'a heading south, although the two maps do not agree on the pattern of the fault. Since not many large lineaments could be interpreted in that area, it is believed that only little groundwater leaves the basin along the southern margin through fractures. In the area between the city of Sana'a and the southern boundary deep

drilling takes place to discover the depth of the sandstones. When this data becomes available and with a survey of the groundwater levels in shallow wells and pressure heads of deep groundwater, more light will be shed on the groundwater flow and possible losses through the deeper layers. .

West
Groundwater flow along the western margin of the basin is more complex to evaluate, because of the presence of the aquifer sandstones (Tawilah) east and west of the volcanic rocks intruded through and extruded over the sandstones. Furthermore, there is narrow rift-Iike structure running north-south. At places, dense irrigation is found at the bottom. It should be noted that the irrigated fields extend only up to the recent lava fields. Also in the southern part no important irrigation is encountered.
The area around Wadi Oahr takes a special place, because of its vincinity to the small N-S running rift structure, just west of it. Apart from lineaments associated with the N-S structure, there are fractures or faults which hydraulic connection of high permeability with the wadi valley. It is therefore possible, that because the drawdown in the wadi has affected the flow pattern to such an extent that groundwater flows in the N-S structure to the wadi.
West of Wadi Dahr a powerful spring was reported to exist, but seems to have dired up by now (Foppen, pers. comrn.). This could confirm a hydraulic connection between the sandstones of Wadi Dahr and their western extension, covered by volcanics. .

Lineaments and artificial recharge
For the selection of artificial recharge sites by small reservoirs, the smaller fractures and master joints are ". of importance in transporting the infiltrated water down into the aquifer. The satellite images are not suitable for identifying the smaller features. They will have to be assessed by using aerial photographs and field studies.
However, no recharge measures are recommended near the margins of the basin in the presence of large lineaments through which groundwater leaves the basin.

8.3 Identification of lineaments on images.

The expression of lineaments on images occurs in various ways:
Straight drainage lines [;
- A fracture has weakened the rocks and increased permeability, so that weathering could take place, ~ preparing preferential paths for fluvial erosion. The incised river follows a straight course.
  Usually, more than one fracturing direction is present, causing the drainage lines to followa sort of diamond shaped pattern.
- Straight narrow valleys could develop in a similar fashion. They are distinct on the image if for example vegetation or irrigation wells are located on the fracture. .

Termination of outcrops along straight lines .
As in field geology, abrupt ending of outcrops along straight lines is taken to be due to faulting or to fracturing. In the latter case the fracture attracted weathering and removal of the products by erosion and solute transport. In uniform, non-layered rocks, such as the volcanics in the Sana'a basin, it is difficult to

assess whether a lineament is associated with a fault or a fracture. - Along the cliffs of the sandstones and limestones, straight edges may be due to presence of master joints or fractures, which do not extend to larger depths. Therefore, only the largest ones have been selected. At places some smaller ones have been included to indicate the presence of a fracture zone.

Straight and curvilinear traces associated with block or step faulting
In areas where the faults can be well mapped because of differential movements off-setting contrasting formations (also spectrally contrasting), such as in the north and west (sandstones-limestones-volcanics), the fault pattern can be studied. In areas where offsets cannot be proven so easily, often faults shown on geologic maps are inferred or suspected (note the large difference in the indication of the faults of the two geologic maps). In the regions around the Sana'a Basin where proven faults exist, the tectonic patterns turns out to be step faulting (in the north) and block faulting in the west (Shibam- Al Mahwit region). Many of the faults in the latter region have limited extensions, and there is considerable variation in the strike of the faults.

The same pattern is observed in the interpreted lineaments of most of the Sana'a Basin. These blocks exist often in the basement, where the displacements can be much more than in the upper levels.
Also they may have been intermittently active and have affected the local geomorphological development. Slight differences in relief due to reactivation of the faults, weathering, erosion and deposition related to micro-relief may have caused linear elements in the terrain. These elements may not be obvious in the field, but become apparent when viewed vertically and at small scale, such as by satellite. Also, the multispectral sensing brings out alignments of features which have different responses, and which correspond to erosional, depositions and microrelief features.

Flexures
Fault movements in the deeper subsurface (basement, Mesozoic rocks) may not result in sharp lineaments at the surface, i.e. in the Quaternary volcanics and alluvial deposits), because of draping over (flexuring). Thus the upward extension of deeper faults could be expressed as faint geomorphological traces. One expects such flexures along extensions of large faults. They have been found in the north-eastern part with the young volcanics, in the continuation of the east west faults off-setting limestones.

Lineaments in the limestones
The lineaments in the limestone region are well visible. They have been drawn using digital enlargements and various processed images. As mentioned, karst may have developed along lineaments. ~ However, not every lineament is associated with permeability .Many of them have slightly different spectral nature as the limestones itself. This could be due to alteration because of weathering and ,. recrystallization (dolomitization, as is shown partially on sheet 15 G). In the latter case the permeability is absent if the crystallization occurred over the full length and depth of the fracture.

Connecting up non-continuous lineament traces
In many cases lineaments are not continuous, but a few of them are found in a single alignment. Some interpreters assume that the fracture (or fault) will be continuous, and will trace the lineament as such.
We have refrained to do so. The tracing is limited to where it could be seen on the images. This does not necessarily mean that there is no connection. The faults shown on sheet 15 G have all been compared with what could be seen on the images. If no traces could be found, they have not been included in the map.

8.4 Image processing and lineaments.

Landsat Thematic Mapper images have been used for the study of the lineaments.

Because of the varied nature of the terrain features that are associated with lineaments, orthogonal decomposition (principal component-PC- transforms) have been applied. This has the advantage that out of the 6 Landsat TM bands, six transformed images result, that are not correlated with each other. The information content, in a statistical sense, decreases rapidly from the first PC to the last. False colour composites of the first three PC's have been used, but it turned out that also PC 4 and PC 5 had their uses for tracing of lineaments.

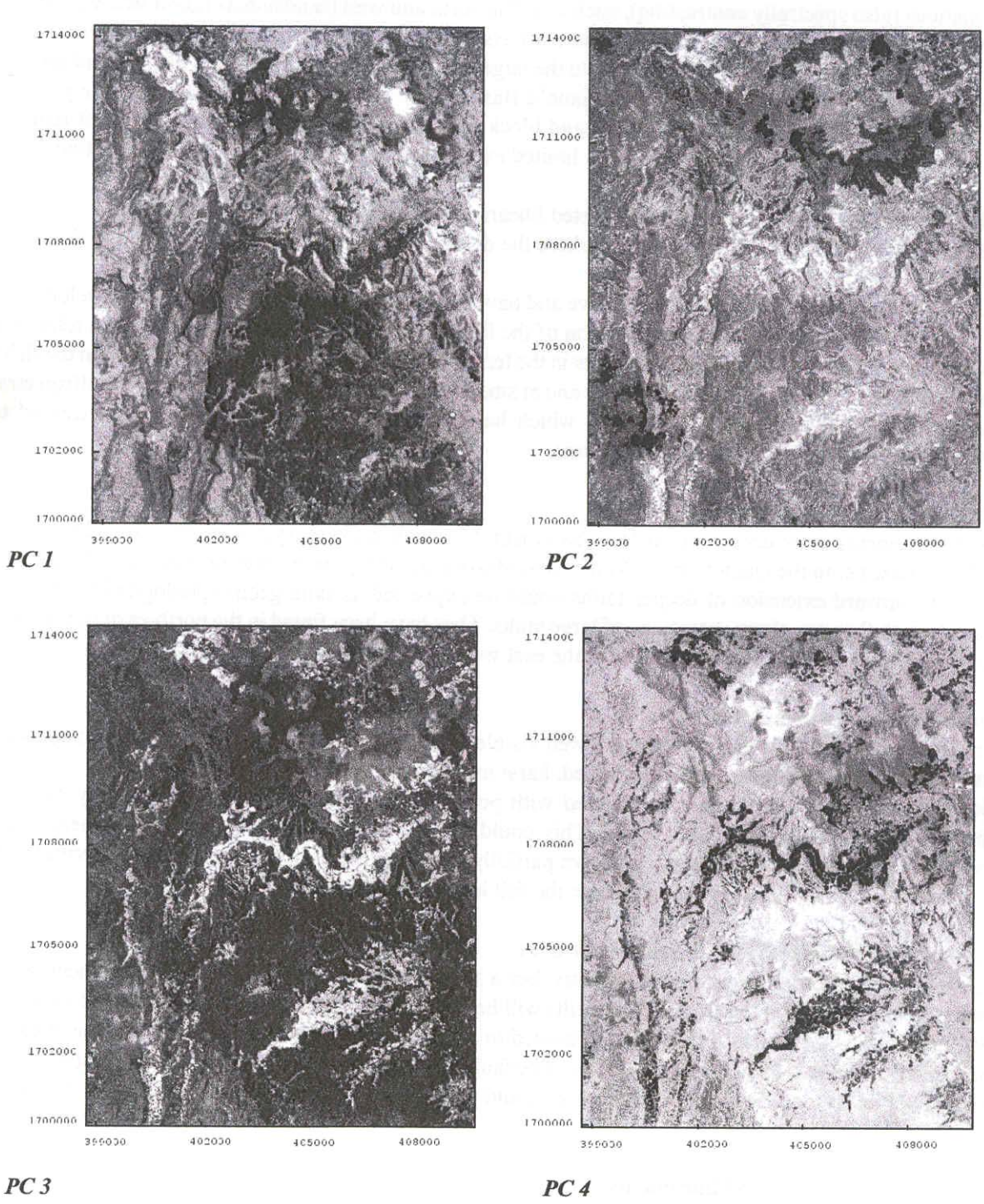

Figure 12. Principal Component (PC) images of the area around Wadi Dhar, Sana'a basin.

The PC images of the area around Wadi Dahr are shown in Figure 12. As can be noted, each image has its own information content.

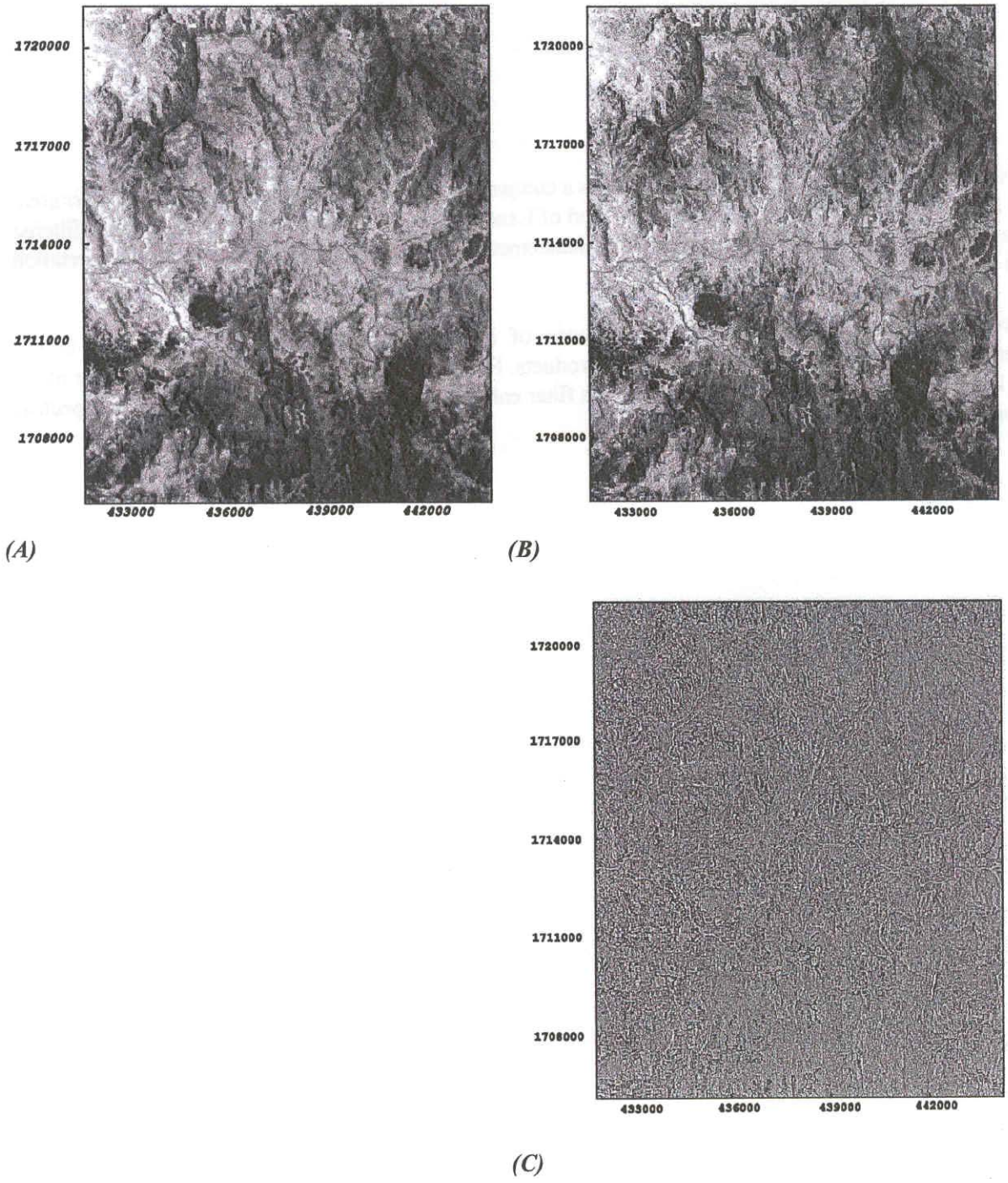

Figure 13. Effects of filtering for enhancements of lineaments; (A) Original TM band 4, (B) Edge enhancement, (C) Laplace filter.

By applying Laplace operators (also known as edge enhancement or high pass filters), linear elements can be visually made more evident. Figure 13 shows a comparison, of the eastern part of the Wadi As Sirr area: (a) is the original image, the near infrared band of Landsat TM, (b) shows the result of a lightly filtered image, as (c) of a strongly filtered image, for enhancement of the contrasts. In all cases visual interpretation has to be done.

Geological, geomorphological and the presence of irrigation has been given more weight in the interpretation than linear elements on filtered products. For the interpretation, asymmetric 3 x3 filter of -I , 8, -I was applied only to the images used. This filter enhances contrasts somewhat but leaves the spectral information of the terrain intact.

9. Hydrogeologic evaluation using irrigation patterns.

The presence of irrigated fields, as apparent from an NDVI transform, involving the infra-red and the red channels of TM, gives an indication of the presence and level of abstraction of groundwater, as well as overall permeability.
The NDVI image of 2000 is shown in Figure 14. White areas are irrigated fields. Medium grey areas correspond to natural (rangeland) vegetation. The rainfall gradient from south west to north-east can be noted, because in the south west medium grey tones predominate.

It is tacitly assumed that allover the basin, the farmers have tried for groundwater by drilling. If no important irrigated are present, then it is supposed that groundwater conditions are poor .

Tertiary volcanics

In the southern and southeastern part of the basin, consisting off ertiary volcanics only, the irrigated areas are not well developed and restricted mainly to the valleys and other topographic depressions, where ignimbrites and ashflows (i.e. pyroclasts) dominate. This is in accordance to the low permeability of the Tertiary volcanics, particularly of the basalts and trachytes. Because of its nature, the pyroclastic deposits have a higher porosity and therefore a higher permeability, in a relative sense.
The sparse irrigation pattern is in accordance with geohydrologic data. Transmissivities were found to range from < 1 m^2/d to 200 m^2/d, but the estimated average permeability ranges, from 0.5 to 1.5 m/d,

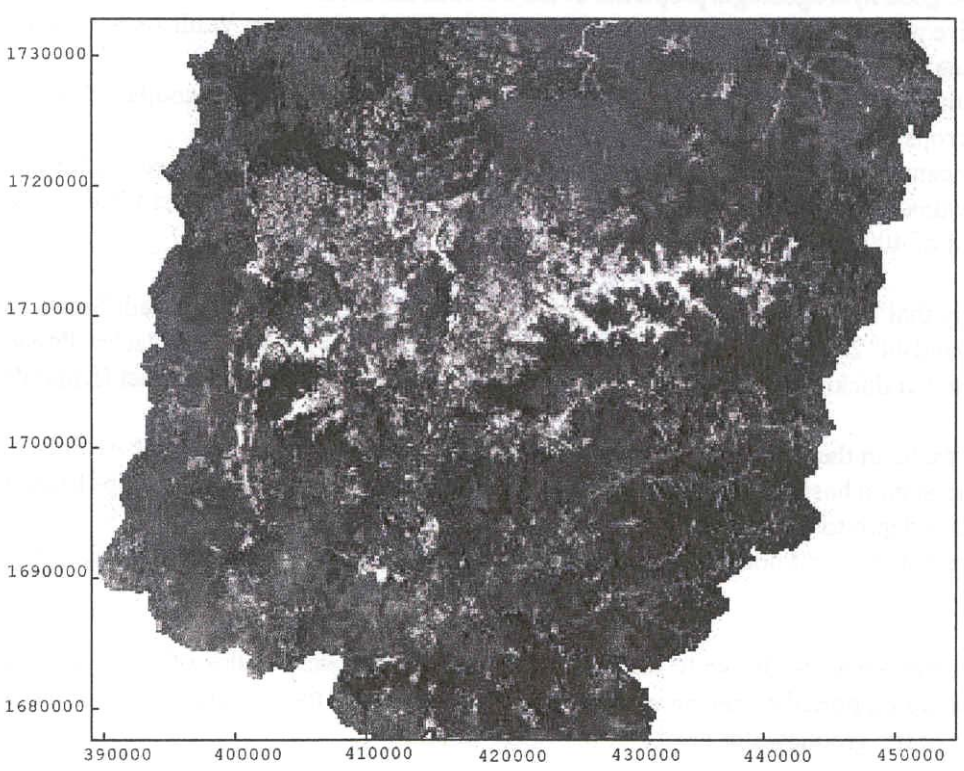

Figure 14. Vegetation index (NDVI) of Sana'a basin, showing presence of are irrigated by groundwater.

according to Foppen (1996). The latter author also mentions that Selkhozpromexport found T values in faultzones in the Tertiary volcanics to be 10 times higher than in fractured zones. In the latter, the

permeability will be substantially higher than in non-fractured zones. Overall porosity for valley alluvium and volcanics was estimated at 1 % only .(SA W AS-2 ,1990, mentioned in Foppen, 1996)
It is therefore likely that wells supplying irrigation water are located on faults and fractures, at low topographic positions to allow flow through the fractures from sections.

Study of the interpreted lineaments and the irrigated fields learns that only a part of the lineaments apparently act as water conduits.

Considering the poor hydrogeologic conditions of the Tertiary volcanic area, it is remarkable that in the area near Hadda (S W of Sana'a city) an important irrigated area is found on the alluvium, surrounded and presumably underlain by Tertiary volcanics. No major faults of fractures could be traced in that area. Foppen (pers. comm.) visited the area and found important spring horizons in the volcanics, which are likely to be associated with permeable pyroclastic layers acting as conduits.

Both available geologic maps show a long fault in Wadi Asfal (10 to 25 km west of Sana'a city). The NDVI image shows hardly a concentration of irrigated fields along the fault. Therefore, it is not likely that the fault is of much hydrogeological importance.

The NDVI image also confirms that some, but no major groundwater losses occur across the boundary of the Sana'a basin.

Cretaceous sandstones

Considering the good hydrogeologic properties of the Tawilah sandstone formation, it is no surprise to find many productive wells (irrigated areas) associated with the sandstone areas: Wadi As Sirr, Wadi Sawan, just east of Sana'a city, Wadi Dhula and Wadi Dahr.
If fact, the southern boundary of dense irrigated fields coincides with generalized southern boundary of the sandstone outcrops.
Quite some lineaments could be traced in these parts, allowing fractured flow through the sandstones. Hence the drawdown could extend much beyond the areas with wells, because in disturbed zones, average transmissivities of 400- 2000 m2/day (in Foppen, 1996).

It is noteworthy that the density and extension of irrigated fields is much less in Wadi Salam (area with sandstones around 44o 27' east, 15° 37' north, east of the road to Marib) and her tributaries. Possible reason could be the limited thickness of the sandstones and proximity of the limestone contact (Karst drainage?)

Similarly, the wadis in the sandstone outcrops west of the Hamdan plateau, south of AI Zufair, (outside the topographic Sana'a basin boundary) have only limited irrigation, which could perhaps be explained by the thickness and depth to groundwater or water quality .
Extensive irrigation is found north of Amran city on alluvium overlaying limestones, according to Sheet 15 G.

Finally, the attention may be drawn to the dense vegetation in the deep valley of Wadi AI Kharid. This vegetation must be supported by spring waters. Further downstream, the vegetation disappears, indicating no intersection of the groundwater level and the valley bottom.

Quaternary volcanics

The pattern of irrigated fields in the terrain underlain by the young volcanic rocks in the north-western part of the basin shows important differences.
It is noteworthy that interspersed irrigation fields are found on the young volcanic terrain, south of the large subrecent lava field (on the road to Amran), till the small NS rift structure is met. Across the structure, no irrigated fields are found.
It is worthwhile to study the subsurface conditions for an explanation, because the recharge in this area cannot support so many wells with a transmissivity of the young volcanics, which is thought to be limited. Possibly the irrigation wells tap sandstones underlying the volcanics and the western boundary is limited by the N-S fault.

Presence of irrigated fields in the N-S structure could point to productive wells in fractured rocks. No such irrigated fields are found along the northern extension of the fault zone. Also in the area NW of the airport,

the irrigated fields disappear to the west and north-west. This could reflect the subsurface configuration of the sandstones underlying the volcanics..

10. CONCLUSIONS AND RECOMMENDATIONS

Conclusions

The study of lineaments has not revealed important faults and fractures showing direct evidence of much loss of groundwater from the Sana'a basin to its surroundings, often at lower altitude.
From a hydrogeological point of view the only possible appreciable loss can occur through deep karst in the northern limestone country .Such losses should be witnessed by large karst springs much further north than the area studied and shown on the NDVI image. If such large springs (outside the area studied on the images) do not exist, the losses could be restricted to the known springs in the upper part of Wadi AI Kharid, unless head conditions make it possible that water flows to the irrigated area north of Amran town through SE-NW trending fracture/fault conduit systems.

By using the extend of irrigated areas as an indicator of groundwater occurrences, it can be noted that the sandstone formations seem to be the most productive in the Sana'a basin proper and not outside the basin. This could indicate that drawdown extends much beyond the well fields because of relatively fast fracture flow through the many existing lineaments.
Once the propagation of the drawdown has reached the limits of the sandstone aquifer, the drop of the water levels in the well fields may accelerate.

In the volcanic area west of Sana'a city, a N-S running structure is found, which has some similarities to a small rift. Available geologic maps show also N-S faulting.
The presence of many irrigated fields east of the fault may point to presence of sandstones below the young volcanics, which could have limited thickness in this area. The small rift-Iike structure could also feed the wells in the sandstones of wadi Dahr. The absence of wells west of the small rift structure is noteworthy.

In the Tertiary volcanic terrain most irrigated areas are found on lineaments, confIrming the poor hydrogeologic conditions. Major faults are not associated with significant irrigation.
It is therefore not likely that the southern part of the Sana'a basin contributes much to the groundwater in the alluvial and the sandstone aquifer in the northern part.
Little loss across the basin boundary can occur in the south-eastern and southern boundary .

Recommendations

Earlier studies have laid the foundation of understanding the groundwater occurrences and hydrogeologic conditions of the Sana'a Basin. However, there are still a number of open questions.

The extension and subsurface extension of the sandstone aquifer is one of them.
The stipulated association of irrigated patterns in the younger volcanics in the west and the configuration of the underlaying sandstones, as mentioned in this study, should be examined by collecting information from drillers, and proper recording of rock types encountered in new wells.

A better insight in the regional subsurface flow patterns is required for the water balance. In this study the attention is drawn to possible gains or losses particularly along the northern boundary of the basin. A survey of the water levels in the area, including wells far beyond the drainage divide of the basin should be done. Such a survey is now feasible by using differential GPS equipment.

The water balance remained so far a matter of crude estimation because of the absence of data. The results presented in Part I of this study has established the amount of groundwater used for irrigation in the entire basin. This data is of direct value for the regional groundwater modelling. The historical trends provides data for transient groundwater modelling.

Data assimilation will improve the knowledge of the hydrogeology of the basin. It is also required as pre-processing for a regional groundwater model. The data types, in the form of maps are:

- Geologic borehole data, re-interpretated and updated, plotted on a map with surface geology .
- Water levels, water level decline

- Hydrochemistry
- Irrigation pattern, actual evapotranspiration (this study)
- Lineaments, relative recharge units (this study)
- Geophysical data, re-interpreted

The vehicle for the data assimilation study is a GIS/RS system with geostatistical and other interpolation software. I ':',

The combination of spatial data yields a host of important products. Just to name a few:

- The water actual evaporation (mm/y) could be divided by the water level decline (mm/y) map. This: represents transmissivity conditions
- A map with groundwater contours (for the flow directions) with the above mentioned product (Eta/water level decline), on a background with the geology (or relative recharge) and lineaments/faults. From that combination possible fracture flow could be deduced.

For selection and evaluation of sites for small dams and / or reservoirs and artificial recharge, use should be made of stereo-aerial photo interpretation, rather than satellite images. ...""

References

Allen R.G., Pereira, L.S., Raes, D., Smith, M 1998. Crop evapotranspiration. Guidelines for computing crop water requirements. F AO Irrigation and Drainage Paper no.56. F AO, Rome.

Bastiaanssen, W.G.M, 1995, "Regionalization of surface flux densities and moisture indicators in composite terrain.", Ph.D. thesis, Agricultural University, Wageningen, The Netherlands, p. 288.

Bastiaanssen, W.G.M, Menenti,M, Feddes, R.A., Holtslag, A.A.M, 1998. A remote sensing surface energy balance equation for land (SEBAL). 1. Formulation Journal ofHydrology vol.212-213, 198-212

Bastiaanssen, W.G.M, Pelgrum, H, Wang, J:, *Ma,JI:,Moreno,J:F., Roerink, G.J., yander Wal, T.* 1998, A remote sensing surface energy balance equation for land (SEBAL). 2. Validation. Journal of Hydrology vol.212-213, 213-229.

Farah, H.O. and Bastiaanssen, W. G *.M* 2001. Derivation of daily evaporation under all weather conditions from standard meterorological data and clear sky flux information. Agriculture and Forest Meteorology, accepted paper, in press.

Foppen, J.A. W. 1996. Evaluation of the effects of groundwater use on groundwater availability in the Sana'a Basin. SAWAS Techn. Rep. no.05, Volume II: Data Availability.
National Water & Sanitation Authority, Sana'a, Yemen & TNO, The Netherlands.

Mekonnen, G.M and Bastiaanssen, W.G.M 2000. Anew simple method to determine crop coefficients for water allocation planning from satellites: results from Kenya. Irrigation and drainage Systems vol. 14, 2000, p 237-256.

Selkhozpromexport, 1985, Sana'a Basin water resources scheme, Vol. 2, Geology and Hydrology, Part 1, 2 and 3. Moscou

Shuttleworth, W.J:, R..J: Gurney, A. JI: *Hsu and .J:P. Ormsby,* 1989, "FIFE: The variation in energy partitioning at surface flux sites.", in Remote Sensing and Large-Scale Global Processes, Proc. Baltimore Symp., IAHS Publ. N°. 186 IAHS press, Oxfordshire, U.K.: 67-74

Appendix.

Plate 1. Crop types.

Plate 2. Crop water use.

Plate 3. Hydrogeological map.

Plate 4. Hydrogeological map, relative recharge.

Available meteorological daily data for ETa calculations. Available meteorological monthly data.

Monthly crop reference evapotranspiration.

Logger data on solar radiation, examples; month, decade. Logger data on atmospheric pressure, examples; month, decade. Field measurements thermal infrared surface temperature. Field traverses, crop classification.

Water use per crop type, per sub-catchment, historical trend.